

Noble gases solubility models of hydrocarbon charge mechanism in the Sleipner Vest Gas Field

P. H. BARRY^{1*}, M. LAWSON², W.P. MEURER², O. WARR¹, J.C. MABRY¹, D.J. BYRNE¹, C. J. BALLENTINE¹

¹ Department of Earth Sciences, University of Oxford, OX13AN, UK

* Corresponding author email: peter.barry@earth.ox.ac.uk

² ExxonMobil Upstream Research Company, Spring, TX, 77389, USA.

For submission to GCA

Number of Words (9,651)

Number of Figures = 9

Number of Tables = 5

August 15, 2016

Abstract

Noble gases are chemically inert and variably soluble in crustal fluids. They are primarily introduced into hydrocarbon reservoirs through exchange with formation waters, and can be used to assess migration pathways and mechanisms, as well as reservoir storage conditions. Of particular interest is the role groundwater plays in hydrocarbon transport, which is reflected in hydrocarbon-water volume ratios. Here, we present compositional, stable isotope and noble gas isotope and abundance data from the Sleipner Vest field, in the Norwegian North Sea. Sleipner Vest gases are generated from primary cracking of kerogen and the thermal cracking of oil. Gas was emplaced into the Sleipner Vest from the south and subsequently migrated to the east, filling and spilling into the Sleipner Ost fields. Gases principally consist of hydrocarbons (83-93%), CO₂ (5.4-15.3%) and N₂ (0.6-0.9%), as well as trace concentrations of noble gases. Helium isotopes (³He/⁴He) are predominantly radiogenic and range from 0.065 to 0.116 R_A; reported relative to air (R_A = 1.4 × 10⁻⁶; Clarke et al., 1976; Sano et al., 1988), showing predominantly (>98%) crustal contributions, consistent with Ne (²⁰Ne/²²Ne from 9.70-9.91; ²¹Ne/²²Ne from 0.0290-0.0344) and Ar isotopes (⁴⁰Ar/³⁶Ar from 315-489). Air-derived noble gas isotopes (²⁰Ne, ³⁶Ar, ⁸⁴Kr, ¹³²Xe) are introduced into the hydrocarbon system by direct exchange with air-saturated water (ASW). The distribution of air-derived noble gas species are controlled by phase partitioning processes; in that they preferentially partition into the gas (i.e., methane) phase, due to their low solubilities in fluids. Therefore, the extent of exchange between

hydrocarbon phases and formation waters – that have previously equilibrated with the atmosphere – can be determined by investigating air-derived noble gas species. We utilize both elemental ratios to address process (i.e., open vs. closed system) and concentrations to quantify the extent of hydrocarbon-water exchange (i.e., volumetric gas-water ratios). These data are discussed within the framework of several conceptual models: i) Total gas-stripping model, which assumes all noble gases have been stripped from the water phase, thus defining the minimum volume of water to have interacted with the hydrocarbon phase; ii) Equilibrium model, which assumes equilibration between groundwater and hydrocarbon phase at reservoir P, T and salinity; and iii) Open and closed system gas-stripping models, using concentrations and elemental ratios. By applying these models to Ne-Ar data from Sleipner, we estimate volumetric gas-water ratios ($\frac{V_g}{V_w}$) between 0.02-0.07, which are lower than standard geologic gas-water estimates of ~0.24, estimated by combining gas-in-place estimates with groundwater porosity estimates. Sleipner Vest data can be best approximated by an open system model, which predicts more than an order of magnitude more groundwater interaction during migration than geologic estimates, indicating a dynamic aquifer system and/or a hydrous migration pathway. In an open system, the extent of gas loss can be estimated to be between 8-10 reservoir volumes, which have passed through the system and been lost (i.e., filled and spilled).

1. Introduction

The principles behind petroleum systems exploration are straightforward but the applications are not; approaches typically require temporal and spatial determination of hydrocarbon source, secondary migration pathways and the occurrence of suitable trapping structures. In practice, each of these parameters within basin systems is multivariate, which together means that most exploration targets are highly complex systems. Basin evolution models provide a temporal framework in which the thermal maturity and timing of hydrocarbon expulsion from source rocks can be predicted. These are dependent on non-linear estimations of subsidence, filling, compaction of sediments and fluids with a range of chemical, physical and mechanical properties over time-scales that can include multiple tectonic processes. Geochemical observations, such as biomarker and stable isotopic information, from surface seeps and subsurface hydrocarbon discoveries are often used to identify source rock and/or maturity information and provide further iteration and confidence in predictive models. There are few techniques that can be used to identify and quantify the controls on secondary migration processes and pathways; noble gases provide such a tool.

The unique and well-defined noble gas isotopic and abundance compositions of different fluid sources (i.e., air-derived, radiogenic and mantle) in sedimentary basins, combined with their chemical inertness, can be used to identify and quantify the physical mechanisms that control interactions between water, oil and gas – thus providing essential information in developing our understanding of petroleum systems (Ballentine et al., 2002;

Prinzhofer, 2013). Noble gases dissolved in water that has equilibrated with the atmosphere – air-saturated water (ASW) – provides the main vector for bringing air-derived noble gases into the subsurface. The unique noble gas isotopic composition of air is preserved in the water but the elemental composition is modified by the differential solubility of the noble gases at recharge or burial (e.g., Kipfer et al., 2002). Atmosphere-derived heavy noble gases (Kr and Xe), can be adsorbed and fixed within carbonaceous sediments, which when released into the fluid system, provides an additional source of these noble gases with an atmospheric isotopic composition (Torgersen and Kennedy, 1999; Zhou et al., 2005).

Contact between groundwater and subsurface oil or gas phases results in the redistribution, or partitioning, of the air-derived noble gases between the different phases. The resulting noble gas composition of each phase is a function of the thermodynamic conditions of the system and the extent and type of contact. In principle, this preserves a record of that interaction in each phase, which has been modelled using different approaches in a number of previous studies (Zartman et al., 1961; Bosch and Mazor, 1988; Zaikowski and Spangler, 1990; Ballentine et al., 1991; 1996; Hiyagon and Kennedy, 1992; Pinti and Marty, 1995; Torgersen and Kennedy, 1999; Schwarzenbach et al., 2003; Zhou et al., 2005; 2012; Gilfillan et al., 2008; 2009; Hunt, et al., 2012; Aeschbach and Solomon, 2013; Darrah et al. 2015). Further information is provided from readily identifiable noble gas nuclides derived from radioactive decay (e.g., ^4He , ^{40}Ar), which can provide temporal constraints. Within open fluid systems the flux of radiogenic isotopes into and out of the fluid system controls their concentration within the fluids (Torgersen and Clarke, 1985; Torgersen and Ivey, 1985; Castro et al., 1998a; 1998b; Zhou and Ballentine 2006; Torgersen 2010). Within closed fluid systems the rate of accumulation in the groundwater (Tolstikhin et al., 1996; Soloman et al., 1996; Cook et al., 1996; Ballentine et al., 2002; Holland et al., 2013) is determined by the solid phase parent radionuclide concentrations and efficiency of release (Tolstikhin et al., 2010; Hunt et al., 2012; Lowenstern et al., 2014; Darrah et al. 2014; Barry et al., 2015) from the mineral into the fluid phase.

Earlier studies of noble gases in hydrocarbon bearing systems have mostly investigated simple models that provide lower limits for groundwater involvement in hydrocarbon migration by assuming total gas stripping of the water phase (e.g., Ballentine et al., 1991), or scenarios in which water and hydrocarbon phases are at simple equilibrium (Ballentine et al., 1996). More recent studies have shown that open system Rayleigh fractionation processes operating on the ASW noble gas signatures can be identified and modelled in coal gas systems to identify both the volume and age of water in contact within this unconventional hydrocarbon system (Zhou et al., 2005). The potential remains to take similar models to conventional hydrocarbon systems to help identify the role of groundwater and style of secondary hydrocarbon migration within conventional oil and gas systems (Hunt et al., 2012; Darrah et al., 2014; Darrah et al., 2015).

In this study, we present noble gas isotope and abundance data as well as major gas compositional and isotopic data from the Sleipner Vest natural gas fields of the Norwegian North Sea (Figure. 1). We have chosen this field because the trapping structure has filled completely and continued gas charging is thought to have caused gas

to spill from this system and charge other nearby accumulations further along the secondary migration path. This is a classic open system 'fill and spill' scenario. Here we develop a series of increasingly more complex models to account for the observed noble gas data. We compare estimates of groundwater involvement assuming: i) Total gas stripping of groundwater to provide a minimum water estimate (zero order model); ii) Equilibration of hydrocarbon and water phases (first order model); iii) Accumulation of the gas in the during groundwater gas stripping at the same time as gas loss via spill (second order, open system model) and iv) Accumulation of the gas in the field due to gas stripping, without gas spill (second order, closed system model). Both closed- and open-system models describe how noble gas concentrations and elemental ratios evolve when the interaction of the hydrocarbons with ASW occurs during migration to the reservoir. Using air-derived noble gas isotopes in our models allows us to understand the extent of exchange between hydrocarbon phases and formation waters. Thus, for the first time, we are able to assess the utility of noble gases in determining the origin and subsequent migration history of gases within this type of hydrocarbon system.

2. Geological background

2.1 Regional Geology and Hydrocarbon Context

The Sleipner Vest field is located in the Norwegian North Sea (Figure 1) at the eastern extent of the South Viking Graben. Natural gas is the dominant form of hydrocarbons within the field, with minor volumes of oil present in the North East of the field. Discovered in 1974, the field is now estimated to contain approximately 6.4 TCF of gas in place (C&C Reservoirs, 2006; Isaksen et al., 2002). Hydrocarbons are hosted in the lower shoreface sandstones of the Jurassic Hugin formation that have a range in thickness from 50 m in the northern part of the field up to 200 m in the central and southern sections of the field (Harris and Fowler, 1987; Husmo et al., 2003; Folkestad and Satur, 2008; Figure 2). The petroleum system is sealed by the Jurassic Upper Draupne and Heather formations. The hydrocarbon gases in this field are thought to represent a mixture of gases generated from primary cracking of kerogen with gases that are derived from the thermal cracking of oil (Isaksen et al., 2002). The likely intervals for these hydrocarbons include the oil prone pre-upper Draupne (dominantly algal marine type II kerogen) and Heather (mixed algal marine and terrestrial type II/III kerogen) source intervals, as well as more gas prone dominantly terrestrial type III Hugin and Sleipner sources. Hydrocarbon migration into the field likely occurred sometime between 70 and 45 Ma, depending on the source interval (Isaksen et al., 2002). The structural relationship between the Sleipner Vest and Ost fields suggests that Sleipner Vest filled from the south and spilled into the Sleipner Ost field to the east (Figures 1 and 2). This setting represents a classic 'fill to spill' gas field, and a primary motivation for targeting it for noble gas characterization. Molecular and gas geochemistry based maturity estimates for the hydrocarbons range from 1.2 – 1.5% vitrinite reflectance equivalence.

3. Methods

3.1 Sample collection

Gases were collected from producing well heads on an offshore platform in the North Sea. At each well location, gases were collected in three separate industry standard 300 cm³ stainless steel (SS) cylinders connected by polytetrafluoroethylene sealed NPT pipe fittings to the wellhead. Cylinders were pre-evacuated, baked and leak-tested prior to being dispatched to the platform for sampling. Cylinders were flushed 5-10 times as to allow the dead space between cylinder and the sampling valve to be adequately flushed. One cylinder from each set was shipped to GeoMark Research LTD in Lafayette, Louisiana, USA for a complete suite of gas analysis. Gas samples were analyzed for stable isotopes and for a complete suite of hydrocarbon gas compositions at GeoMark using standard techniques as described in Zumberge et al., 2012. The remaining two cylinders were shipped to the University of Oxford, Oxford, UK for noble gas analysis.

3.2 Analytical techniques

Noble gas analysis was conducted in the Noble Laboratory at the University of Oxford using a dual mass spectrometer setup, interfaced to a dedicated hydrocarbon extraction and purification system. Gases were decanted (within one month of arrival at Oxford) from the SS cylinders and sub-sampled in refrigerator-grade 10 mm outside-diameter Cu-tubes at <1.5 atm pressure, using an offline vacuum transfer line. Approximately 40 cm³ (STP) of the sub-sample was then transferred to the extraction and purification line where hydrocarbons and reactive gases were chemically removed by exposing gases to a titanium sponge held at 800 °C. The titanium sponge was cooled for 30 minutes to room temperature in order to getter hydrogen before gases were expanded to a dual hot (SAES GP-50) and cold (SAES NP-10) getter system, held at 250 °C and room temperature, respectively. A small aliquot of gases was segregated for preliminary analysis on a Hiden Analytical HAL-201 quadrupole mass spectrometer. Purified gases were then passed through a stainless steel water trap held at 180 K. The sample noble gases were separated using a series of cryogenic traps which were cooled using helium compressors. The heavy noble gases (Ar-Kr-Xe) were adsorbed at 15 K onto an all SS trap and the Ne was adsorbed at 31 K on a charcoal trap, leaving only He, which was then inlet into a Helix SFT mass spectrometer. Following He abundance and isotope determination, the temperature on the charcoal cryogenic trap was raised to 90 K for fifteen minutes to release Ne, which was inlet into an ARGUS VI mass spectrometer. Following Ne isotope measurement, the SS cryogenic trap temperature was raised to 300 K and a small aliquot of Ar-Kr-Xe was isolated and inlet into the ARGUS VI in order to determine their relative elemental abundances and Ar isotopes. The remaining (>99%) heavy noble gases were then re-adsorbed onto the SS cryogenic trap at 15 K. The temperature was then raised to 200 K for transfer of Kr and Xe to a third cryogenic (charcoal) trap held at 180 K on the

extraction line. Following transfer of heavy noble gases, the line was pumped for an additional 15 minutes to remove any residual Ar. The cryogenic trap was then raised to 375 K for one hour to ensure complete release of Kr and Xe. Both gases are simultaneously inlet into the ARGUS VI, but only Xe isotopes are analyzed upon the initial expansion. The residual gas remaining in the preparation line is then inlet into the ARGUS VI for Kr isotope determination.

Full ‘procedural blanks’ were run weekly; average (mean) ^4He blanks were 0.45% of the average (Sleipner Vest) sample size, ^{20}Ne blanks were 0.65%, ^{36}Ar blanks were 1.10%, ^{84}Kr blanks were 0.23% and ^{132}Xe blanks were 0.25%, and thus blank corrections were typically less than 1%. Doubly-charged $^{40}\text{Ar}^{++}$ corrections were applied to ^{20}Ne data following the methods of Niedermann et al., 1993; however no CO_2^{++} correction was applied to ^{22}Ne due to the fact that CO_2 backgrounds were at the detection limit and thus corrections were considered insignificant.

‘External air-standards’ were also run once per week from an air cylinder collected in University Parks, Oxford, UK on November 24, 2014 (Temperature: 4°C, humidity: 95%, pressure: 1027hPa). Weekly air-standards were calibrated against ‘internal running-standards’, which were run each night following sample analysis. He, Ne, Kr and Xe running standards were purified from a stock air tank provided by Thermo Fisher, following the procedures described above, whereas Ar running standards were run from a pre-cleaned stock Ar-tank, also provided by Thermo Fisher. Running-standards were fully automated and run overnight, following sample analysis during the day. Standards were run for all noble gas isotopes and they were determined over a large concentration range, which spanned two orders of magnitude, as to ensure that samples of any size could be normalized to similar sized standards.

4. Results

4.1 Major volatiles and stable isotopes

The major Sleipner Vest gases (n=12) are comprised of hydrocarbons (69-80% C1; 8-9% C2 and 4-5% C3), CO_2 (5.4-15.3%) and N_2 (0.6-0.9%); compositions are given in Table 1. Methane (CH_4) and CO_2 show a strong negative correlation ($R^2 = 0.94$ for ‘Normal Samples’; Figure 3). The carbon isotopic $\delta^{13}\text{C}$ composition of CO_2 , spans a limited range between -8.3 and -6.7‰ (measured relative to Vienna Pee Dee Belemnite (VPDB)) forming a weak positive correlation ($R^2 = 0.38$) with CO_2 concentration, with the most negative value measured in the lowest CO_2 sample. Carbon isotope values of hydrocarbon gases also span a limited range in values over the field. Methane $\delta^{13}\text{C}$ (C1) ranges from -40.9 to -38‰, ethane $\delta^{13}\text{C}$ (C2) ranges from -29.3 to -28.0‰ and propane $\delta^{13}\text{C}$ (C3) ranges from -27.4 to -27.0‰ vs VPDB. Maturity estimates (1.2 to 1.5% vitrinite reflectance) based on the isotopic signatures of ethane and propane suggest source rock depths and temperatures greater than 5 km and 160 °C respectively (Isaksen et al., 2002).

4.2 Noble gases

The majority of the samples ($n=9$) have relatively consistent noble gas concentrations, whereas three 'Outlier Samples' (B-02, B-03, B-05) are higher by a factor of 10. We suggest that the three outlier samples are most-significantly air contaminated (air $^{20}\text{Ne}/^{36}\text{Ar} = 0.50$). Measured $^{20}\text{Ne}/^{36}\text{Ar}$ values range from 0.127 to 0.273 in the majority of 'Normal Samples' and from 0.462 to 0.567 in the outlier samples. Sample B-06 has the highest $^{40}\text{Ar}/^{36}\text{Ar}$, $^{21}\text{Ne}/^{22}\text{Ne}$ (Figure 4) and lowest $^{20}\text{Ne}/^{36}\text{Ar}$ of all samples measured in Sleipner Vest; whereas the highest $^{20}\text{Ne}/^{36}\text{Ar}$ value measured (i.e., outlier sample B-02) has an air-like $^{20}\text{Ne}/^{36}\text{Ar}$ ratio and the lowest $^{40}\text{Ar}/^{36}\text{Ar}$ and $^{21}\text{Ne}/^{22}\text{Ne}$. In figure 5b we plot $^{21}\text{Ne}/^{22}\text{Ne}$ vs. $^{20}\text{Ne}/^{36}\text{Ar}$ and show that the highest (most nucleogenic) neon isotope ratios are associated with the lowest $^{20}\text{Ne}/^{36}\text{Ar}$ and that even the normal samples exhibit some contribution from modern air, most likely contamination during sampling or storage. Similarly, measured $^4\text{He}/^{20}\text{Ne}$ values range between 2478 and 8270, all of which are significantly higher than the ASW value of 0.288 in groundwater (e.g., Kipfer et al., 2002), showing that atmosphere-derived He contributions are negligible in all cases. Notably, the outlier samples (i.e., B-02, B-03, B-05) have significantly lower $^4\text{He}/^{20}\text{Ne}$ values of ~ 500 , lending further credence to the hypothesis that these samples have been proportionately modified by air. Sample B-06 has the highest measured $^4\text{He}/^{20}\text{Ne}$ value, again consistent with this sample being the least affected by modern air contamination.

The outlier samples are not geographically distinct, nor were they analysed consecutively; however, they are numerically consecutive (note: well B-04 was not sampled). We surmise that these samples became contaminated during sample collection. We note that all the samples were collected using industry standard collection vessels and collection protocols designed for major composition and stable isotope determination and not the more rigorous collection techniques usually adopted by the noble gas community for noble gas determination (e.g., Aeschbach-Hertig and Solomon, 2013). For the purpose of describing the observed ranges in individual noble gas species, we only present the concentration range in 'Normal Samples'. As noted, sample B-06 has the lowest measured air-derived noble gas concentrations of all 'Normal Samples' as well as the highest (i.e., most pristine) $^{40}\text{Ar}/^{36}\text{Ar}$ (Fig. 5) and $^{21}\text{Ne}/^{22}\text{Ne}$ (Fig. 6). If small amounts of air-contamination are endemic to our samples, then B-06 is least affected and thus most representative of the hydrocarbons in this gas field.

Helium (^4He) concentrations range from 53.2 to $68.1 \times 10^{-6} \text{ cm}^3\text{STP}/\text{cm}^3$; samples are strongly radiogenic and have helium isotope ($^3\text{He}/^4\text{He}$) values ranging between 0.065 ± 0.002 and $0.116 \pm 0.003 R_A$, reported relative to the air value $R_A = 1.39 \times 10^{-6}$ (air = $1R_A$; Clarke et al., 1976; Sano et al., 1988). All noble gas data are reported in table 2 along with 1σ uncertainties. Variations in $^3\text{He}/^4\text{He}$ ratios correspond to minor, but resolvable, mantle He contributions. Using a simple two-component mixing model between sub-continental lithospheric mantle-like ($6.1 R_A$) and crustal ($0.007 R_A$) endmembers (e.g., Ballentine and Burnard, 2002; Day et al., 2015), then the percentage crustal radiogenic ^4He varies between 98.2 and 99.0% and we neglect discussion of mantle derived noble gas sources in the remainder of this particular contribution.

Neon (^{20}Ne) concentrations range from 7.1 to $26.8 \times 10^{-9} \text{ cm}^3\text{STP/cm}^3$. Sleipner Vest samples show minor deviations from the atmospheric $^{20}\text{Ne}/^{22}\text{Ne}$ value of 9.8 , potentially due to a small mantle contribution or a small amount of fractionation. Measured $^{20}\text{Ne}/^{22}\text{Ne}$ ratios vary between 9.70 ± 0.008 and 9.91 ± 0.008 . Measured $^{21}\text{Ne}/^{22}\text{Ne}$ ratios vary between 0.0309 ± 0.0001 and 0.0344 ± 0.0001 . $^{21}\text{Ne}/^{22}\text{Ne}$ isotopic ratios in excess of the air value (0.0290) can be accounted for by crustal radiogenic ^{21}Ne addition to air-like Ne. Samples with the lowest $^{21}\text{Ne}/^{22}\text{Ne}$ appear to have been proportionally modified by air-contamination (Figure 4b).

Argon (^{40}Ar) concentrations range from 27.2 to $40.7 \times 10^{-6} \text{ cm}^3\text{STP/cm}^3$ and reveal significant deviations from the atmospheric $^{40}\text{Ar}/^{36}\text{Ar}$ value of 298.56 (Lee et al., 2006), with measured $^{40}\text{Ar}/^{36}\text{Ar}$ values varying between 315 ± 1.57 and 488 ± 2.44 . These values show a resolvable contribution from a ^{40}Ar -rich source. In the absence of significant mantle-derived helium, we assume this is derived from crustal radiogenic sources within the petroleum system. Measured $^{38}\text{Ar}/^{36}\text{Ar}$ values are predominantly air-like (0.1885 ; Lee et al., 2006; Burnard, 2013) and vary between 0.183 ± 0.002 and 0.188 ± 0.002 . $^{40}\text{Ar}/^{36}\text{Ar}$ values are correlated to ^{20}Ne concentrations (Figure 4a), consistent with small amounts of air contamination in the samples with the lowest $^{40}\text{Ar}/^{36}\text{Ar}$.

Krypton (^{84}Kr) concentrations range from 2.94 to $4.01 \times 10^{-9} \text{ cm}^3\text{STP/cm}^3$. The samples are air-like (0.3032 ; Aregbe et al., 1996) with respect to $^{86}\text{Kr}/^{84}\text{Kr}$, ranging between 0.302 ± 0.003 and 0.308 ± 0.003 , (Table 2).

Xenon (^{132}Xe) concentrations range from 338 to $410 \times 10^{-12} \text{ cm}^3\text{STP/cm}^3$. Xenon isotope ($^{132}\text{Xe}/^{130}\text{Xe}$) ratios are air-like (6.60705 ; Pepin, 2000), ranging between 6.5803 ± 0.0165 and 6.6239 ± 0.0166 , (Table 2).

5. Discussion

Using conventional geochemical tools such as molecular geochemistry, vitrinite reflectance and visual kerogen analysis, information about the source rock kerogen type, age, and thermal maturity can be gleaned from many oil accumulations. Stable isotope geochemistry and bulk composition of hydrocarbon gases provide similar but less robust constraints for gas accumulations. While recent developments in clumped isotope geochemistry give new insights into the temperatures associated with hydrocarbon formation (e.g., Stolper et al., 2014), these techniques provide essentially no information about the important process(es) associated with secondary hydrocarbon migration through the hydrocarbon system from the source environment to the reservoir and beyond. In the following discussion we use the noble gas composition of the hydrocarbon gases to test models of open- versus closed-system behaviour. The noble gases can also be used to estimate the relative proportions of hydrocarbon to ASW that they interacted with. Knowledge of hydrocarbon volumes in subsurface accumulations is the primary metric that drives commerciality of any discovery. However, assessment of connected water volumes may also be useful when considering the nature of aquifer support for hydrocarbon production, and this can

substantially influence the economic viability of an accumulation. The Sleipner Vest field is well-characterized and provides an ideal setting to contrast model results with observations.

5.1 Origin of atmospheric noble gases

Atmospheric-derived noble gases (i.e., ^{20}Ne , ^{36}Ar , ^{84}Kr and ^{132}Xe) are transported into the subsurface dissolved in water during aquifer recharge and/or during burial of air saturated pore fluids. Air-derived noble gases have no significant subsurface source, in contrast to radiogenic and/or mantle derived noble gas isotopes. The unambiguous origin of ASW derived noble gases provides great utility when assessing hydrocarbon migration and storage. The initial ASW noble gas inventory in pore-fluids can be estimated using solubility data; noble gas solubility in water is temperature and salinity dependent, but generally increases with mass ($\text{Ne} < \text{Ar} < \text{Kr} < \text{Xe}$), thus ASW noble gas values vary as a function of recharge conditions (temperature, salinity and recharge elevation). In Sleipner Vest we assume recharge conditions of 10 °C and 0.623 M NaCl from relict North Sea recharge waters at sea-level. The initial noble gas inventory was acquired during marine deposition and subsequently isolated from further groundwater inputs. Noble gas exchange occurs during hydrocarbon migration and will dictate the final noble gas inventory of the hydrocarbons phase. For example, in Sleipner Vest, the reservoir is at a depth around 3535 m and has a temperature of 88 °C; however, the source is at a depth between 5000-6000 m, providing a wide range of conditions under which noble gases can exchange. Within the reservoir, additional partitioning can potentially take place, particularly if formation water flows past the static hydrocarbon phase within reservoir rocks to provide an additional source of noble gases. Noble gases can also be lost from the system either prior to (open and then closed system) or after the structure is filled (fill and spill). Noble gas signatures in hydrocarbons can be modified through fluid-rock interaction (Section 5.4), whereby sediments that have a sorbed inventory of (heavy) noble gases partition into the hydrocarbon phase (e.g., Zhou et al., 2005). These processes could operate sequentially or, in some cases, simultaneously and thus potentially complicate interpretation of measured hydrocarbon signatures. The predicted geochemical consequences of these scenarios on noble gas signatures are discussed here.

5.2 Gas water volume estimates

5.2.1 Geologic Gas/water estimates

Noble gases can potentially reveal important information about the extent of hydrocarbon-water interaction, and thus provide valuable insight into hydrocarbon migration pathways, storage mechanisms and reservoir conditions. A useful way to quantify the extent of interaction is to calculate the extent of gas-water

interaction (i.e., volumetric gas/water ratios) for a given hydrocarbon reservoir, which forms a useful comparison with static gas in place to water estimates.

In Sleipner Vest, static ‘geologic’ volumetric gas/water ratios were calculated by integrating information from well logs and depth maps for the Hugin reservoir and the underlying Sleipner interval. Volumetric calculations for both *in-situ* gas and water were based on measurements of porosity (18%), well logs for residual water saturation, and total average thickness (150m) of sand relative to non-reservoir rock (net to gross) based on seismic data. Gas volumes were estimated based on the porosity above the free water level (mapped across the field from well penetrations) minus that occupied by residual water. Free water level represents the depth below which you transition from dominantly gas saturated pore space to dominantly water saturated pore space. Similar estimates were made for water-saturated intervals below the free water level. An additional volume of water equivalent to that displaced by the gas was added to the water volume below the free water level. This estimate considers only gas and water present in the Hugin reservoir interval for the area of the field down to the synclinal spill point at the eastern and western margins of the field beyond which no seismic data was available. Using this approach, we estimate a static ‘geologic’ volumetric gas-water ratio of approximately ~0.24 at reservoir temperature and pressure (RTP). The gas/water volume ratio derived provides a reference frame for assessing the gas/water ratio derived from the gas phase noble gas composition.

5.2.2 Noble Gas constrained Gas/Water estimates

In this section we present the noble gas results from Sleipner Vest within the framework of four conceptual models: i) Zero order model: Total gas-stripping – this defines the minimum volume of water to have interacted with the hydrocarbon phase; ii) First order model: An equilibrium model that assumes simple equilibration between groundwater and hydrocarbon phase at reservoir conditions; iii) Second order models: a) Open system gas-stripping and b) Closed system gas-stripping models, where the phrase ‘gas stripping’ refers to the partial extraction of noble gases from ASW due to interaction with a hydrocarbon phase, according to Henry’s law (Table 3). Such models can be used to understand the production, migration history and storage mechanisms of noble gases in the Sleipner Vest field.

All noble gas models assume that sample B-06 is most representative of the Sleipner Vest reservoir gas composition and thus is best suited to model $\frac{V_g}{V_w}$ ratios. All models assume that measured non-radiogenic noble gas isotopes in the hydrocarbon gas (i.e., methane) are derived from interaction with ASW and that there is no significant cross formational flow of noble gases since hydrocarbon charge. Models also assume ideality in the gas phase, however in dense methane-water systems there may be a small degree of deviation from ideal behavior for noble gases (Warr et al., 2015). In all models, partition coefficients at depth are based on reservoir pressure (400

bar), temperature (assumed to be 88 °C) and salinity (1.2 M NaCl), while those for the air-water partitioning at groundwater recharge conditions (i.e., temperature and salinity), are assumed to be 10 °C and seawater (0.623 M NaCl) at 1.01 bar. Importantly, model outputs are relatively insensitive to recharge assumptions; for example, if recharge temperatures and salinities are varied by a factor of two, it results in little difference (~3%) on the final $\frac{V_g}{V_w}$ that we calculate. As such, like previous studies we assume that the dominant phase of noble gas exchange between formation waters and hydrocarbons occurs in the reservoir intervals. This is not unreasonable given that these lithologies preserve the highest porosity and therefore host the largest volumes of formation water of any element (e.g., source, migration pathway and reservoir) within the hydrocarbon system. Exchange during hydrocarbon migration through previous reservoirs, in traps upstream of the sampled accumulation, is possible, but quantifying this is beyond the scope of these models, because of significant uncertainty in the conditions of migration, among other factors.

5.2.3 Zero Order (ZO) Total Gas Stripping Model

The total gas-stripping model assumes quantitative degassing (i.e., total gas stripping) of the initial water body. This represents an endmember scenario in that 100% of noble gas *i* has effectively been removed from the water phase and is now in the gas phase. This model estimates a minimum volume of water (V_w) necessary to produce the measured gas concentrations [$C_{i(meas)}^g$] (all concentration units are cm³STP/cm³), and thus results in the highest $\frac{V_g}{V_w}$ of any model. All parameters used in the equations below are defined (Table 4). We use the abbreviation (**ZO**) to indicate the zero order and write the equation in the form of:

$$\frac{V_g}{V_w}(\mathbf{ZO}) = \frac{[C_i^{asw}]}{Z[C_{i(meas)}^g]} \quad (1)$$

Where [$C_{i(meas)}^g$] and [C_i^{asw}] are concentrations of noble gas *i* in the measured gas phase and the initial ASW, respectively and $\frac{V_g}{V_w}$ is the unit-less volumetric gas to water ratio under reservoir temperature and pressure (RTP). Gas concentrations are measured at standard temperature and pressure (STP), and thus we use a compression factor (Z) that enables conversion from STP to RTP, where STP = 273.15 K at 1 bar.

$$Z = \frac{[273.15 P_R]}{T_R} \quad (2)$$

Where P_R = discovery reservoir pressure (bar) and T_R = reservoir temperature (K).

Working through the calculation for $\frac{V_g}{V_w}(\mathbf{ZO}^{20}\text{Ne})$: air saturated seawater at 10 °C contains $\sim 1.51 \times 10^{-7}$ cm³STP/g and [^{20}Ne] of sample B-06 is $\sim 7.06 \times 10^{-9}$ cm³STP/cm³. In order to produce this [^{20}Ne] in 1 cm³ of gas at STP requires approximately 0.047 cm³ of water to be completely stripped of its initial noble gas inventory. Because this model assumes total gas stripping, it does not require the use of Henry's constants beyond calculating the

initial ^{20}Ne content of the groundwater. Notably, all $\frac{V_g}{V_w}$ ratios reported here are at RTP. To convert $\frac{V_g}{V_w}$ (ZO^{20}Ne) at STP to RTP conditions, we apply a compressibility factor (Z). Sleipner discovery well pressures and temperatures were ~400 bar and ~88 °C. As a result, the gas phase is compressed by a factor of approximately 302, whereas the water phase is assumed to be incompressible, thus resulting in reservoir $\frac{V_g}{V_w}$ (ZO^{20}Ne) = 0.071. The same approach is used for ^{36}Ar , ^{84}Kr and ^{132}Xe (Table 5).

5.2.4 First Order (FO) Equilibrium Model

The equilibrium model assumes that the produced hydrocarbon phase is in direct contact with the water and that equilibrium has been reached at reservoir conditions. This would represent a scenario where hydrocarbons fill a trap through displacement of formation water and equilibrate at the gas-water contact within the reservoir interval. Under these conditions a quantifiable portion of the initial noble gas inventory remains dissolved in the water. Therefore this model requires a larger volume of water to produce the measured gas concentrations relative to the zero order (ZO) model.

In the first order (FO) equilibrium model, we simply calculate $\frac{V_g}{V_w}$ (FO) by modifying eq. 1 to include a term 'H', which adjusts the gas water ratio to account for the fraction of noble gas i re-dissolved in the water:

$$\frac{V_g}{V_w} (\text{FO}) = \frac{[C_i^{\text{asw}}]}{Z[C_{i(\text{meas})}^g]} - H \quad (3)$$

H is defined as:

$$H = \frac{22400 T_R \rho_w}{1000 \times 273.15 K_i^M} \quad (4)$$

Where one mole of an ideal gas at STP occupies 22400 cm³, T_R is the reservoir temperature (K), ρ_w is the density of water and K_i^M is the reservoir temperature and salinity specific Henry's constant (Crovetto et al., 1982; Smith and Kennedy, 1983; Smith, 1985). In this way we can calculate $\frac{V_g}{V_w}$ (FO) under reservoir conditions using just the measured gas concentration $[C_{i(\text{meas})}^g]$. Employing this approach, we calculate a $\frac{V_g}{V_w}$ (FO^{20}Ne) of 0.061 for Sleipner Vest. The same approach is used for ^{36}Ar , ^{84}Kr and ^{132}Xe (Table 5).

5.2.5 Second Order (SO) Open System Degassing Model

We now consider an open system model that assumes there is partial loss of hydrocarbons from the system. The model initially assumes that a small volume of gas (G) equilibrates with a much larger static water

volume (W), containing ASW concentrations of noble gas (C_i^{asw}), during displacement of formation water from the reservoir in a trap. Once the gas has reached the trap the model assumes negligible interaction (i.e., rates of advective and diffusive exchange at the gas-water contact are insignificant). In contrast to the closed system model, it is assumed that gas is lost. For example, this loss could be associated with hydrocarbon migration prior to the development of the trapping structure or competent seal, resulting in loss from the reservoir formation. Alternatively, this may represent a scenario where hydrocarbons are lost following filling the trap to the point of spilling. In the latter case this will result in a 'fill and spill' process wherein the latest gas can displace the earlier gas charge. In these scenarios the concentration of the water evolves according to a Rayleigh distillation. As hydrocarbons (and noble gases) are progressively lost from the reservoir, measured concentrations in both the gas and water phase tend towards zero.

We begin by calculating how ASW with an initial number of moles of noble gas i (n_i^{asw}) will evolve in an open system as gas stripping progresses. We calculate the total number of moles remaining in the residual water (n_i^w) after 'd' degassing steps:

$$n_i^{asw} = n_i^w F^d \quad (5)$$

Where F is the term that describes the relative partitioning between an assumed volume of gas 'G' and water packet 'W' and F^d is the fraction of noble gas i which remains in the water phase [n_i^w] following 'd' gas stripping steps, at a given Henry's constant K_i^M . If G is infinitesimally small relative to W, F approaches 1 (i.e., a very small bubble strips a relatively small amount of gas from ($n_i^{asw_0}$)). The F value can be defined as:

$$F = \frac{H}{H + \frac{G}{W}} \quad (6)$$

Based on the known concentration of noble gases in ASW, and one mole of an ideal gas occupying 22400 cm³ we can calculate the number of moles [n_i^{asw}] in a given volume of water (W):

$$n_i^{asw} = \frac{WC_i^{asw}}{22400} \quad (7)$$

Taking the measured gas concentration [$C_{i(meas)}^g$], we can calculate the number of moles [n_i^w] in a given water (W) volume following 'd' degassing steps that are required to impart this gas concentration into a given gas (G) volume.

$$n_i^w = C_{i(meas)}^g \left(\frac{P_R}{K_i^M} + \frac{ZG}{22400} \right) \quad (8)$$

In this equation it is critical to determine how much degassing/gas stripping must have occurred to impart the noble gas signature on our sample. Therefore, we rearrange equation 5 and solve for 'd' to get:

$$d = \frac{\ln\left(\frac{n_i^w}{n_i^{asw}}\right)}{\ln(F)} \quad (9)$$

If we then substitute the solutions from equations 6-8 into equation 9, we can solve for 'd' at a measured noble gas concentration $[C_{i(meas)}^g]$. We can then plug in the solution from equation 9 into equation 10 along with the assumed G and W volume values to solve for $\frac{V_g}{V_w}$ (**SO Open**), in the reservoir under open system conditions:

$$\frac{V_g}{V_w} (\text{SO Open}) = \frac{dG}{W} \quad (10)$$

Open system elemental ratio volumetric $\frac{V_g}{V_w}$ (**SO Open ER**) estimates

Due to the fact that individual noble gas nuclides have different solubilities, elemental ratios will evolve in a predictable way as gas progressively strips the noble gases out of the water phase. Conceptually, the earlier volumes of gas to reach the trapping structure will have higher concentrations of ASW-derived noble gases, and will be enriched in the least soluble noble gases relative to ASW. As gas processing of the static water volume proceeds, each volumes of gas that migrates through the water body will have lower ASW noble gas concentrations and their elemental composition will reflect the preferential removal of the least soluble noble gases from the water phase by earlier gases. Therefore, the gas composition (i.e., elemental ratio) reflects the extent to which the original ASW content has evolved and the required volume of gas that must have passed through the water body required to effect this change. In an open system scenario, where earlier batches of noble gases escape, highly fractionated relative elemental ratios can be achieved as mass balance is not preserved. The calculated volumetric gas to water ratio $\frac{V_g}{V_w}$ (**SO Open ER**) is therefore the total volume of gas that must have equilibrated with the water body prior to sample collection.

Using a traditional open system approach (e.g., Zhou et al., 2005), we can calculate the evolution of any two individual noble gas species (i and j) relative to one another as gas stripping progresses, and thus calculate an independent $\frac{V_g}{V_w}$ for any measured elemental ratio (i/j) . In an open system, the initial extremum elemental ratio (i/j) is controlled by the relative solubility coefficients between i and j. The "first bubble" is defined as the point at which the saturation limit of methane is exceeded and a free gas phase forms in the subsurface. The first bubble starting extremum value (i.e., $\frac{V_g}{V_w} \rightarrow 0$) is defined by the equation:

$$(i/j)_{\text{"1st bubble"}} = \frac{K_i^M [(i/j)_{asw}]}{K_j^M} \quad (11)$$

As gas stripping proceeds, $\left(\frac{i}{j}\right)$ the gas phase will continuously fractionate according to a Rayleigh distillation towards a limit (i.e., zero or infinity). By modifying eq. 10, the $\frac{V_g}{V_w}$ can be estimated at a measured $\left(\frac{i}{j}\right)$ using the following equation:

$$\frac{V_g}{V_w} (\text{SO Open Elemental Ratio}) = \frac{G}{W} \left(\frac{\ln \left(\frac{\left(\frac{i}{j}\right)_{meas}}{\left(\frac{i}{j}\right)_{asw}} \right)}{\ln \left(\frac{F_i}{F_j} \right)} \right) \quad (12)$$

The fact that B-06 has a $^{20}\text{Ne}/^{36}\text{Ar}$ value below ASW strongly suggests that the system is open and approaching a scenario whereby all noble gases have been quantitatively degassed from the groundwater into the gas phase. If the system were closed to gas loss, then gases could not evolve to $^{20}\text{Ne}/^{36}\text{Ar}$ values below the ASW value (Figure 6) due to Ne being less soluble in the water phase relative to Ar. The fact that sample B-06 does evolve below this point (Figure 7; Figure 8a), strongly suggests that the Sleipner Vest system is open (i.e., fill and spill scenario).

5.2.6 Second Order Closed System Degassing Model

The closed system model assumes that the hydrocarbon gases interact with ASW, migrate away and remain isolated in the reservoir. We assume that in the first instance a small volume of gas (G) equilibrates with a static water volume (W), initially containing ASW concentrations of noble gas (C_i^{asw}). Once the gas reaches the trap this model assumes negligible additional exchange at the gas-water contact and there is no loss of gas from the trap. Subsequent volumes of gas passing through and equilibrating with the same water then reach and are stored in the same trap, where they mix with previous volumes of gas. Notably, a perfect seal is unlikely to exist in reality, however for the purpose of our hypothetical closed system model, we consider the extent of loss to be negligible, certainly when compared to an open system (fill and spill type) model. The noble gas content measured in a trapped gas is the net result of this 'closed system' process. Conceptually, the earlier volumes of gas to reach the reservoir will have higher concentrations of noble gases, and will be enriched in the least soluble noble gases relative to ASW. As gas filling of the reservoir proceeds, subsequent volumes of gas will have progressively more dilute noble gas concentrations and their elemental composition will reflect the preferential removal of the least soluble noble gases from the water. As noble gas concentrations in the water phase approach zero, the elemental ratios of the gas in the trap will approach ASW. Continued addition of gas migrating through the same water will simply reduce the concentration of the noble gases in the reservoir. The gas to water ratio recorded by the noble

gases in the ‘closed system model’ is the total volume of gas now in the reservoir relative to the total volume of water the gas equilibrated with during its ascent.

In the closed system model all hydrocarbons are trapped and well-mixed, and the noble gas composition of the gas evolves according to the relative partition coefficients of the individual noble gas species. In this way we can calculate a $\frac{V_g}{V_w}$ (**SO Closed**), using a measured noble gas concentration $[C_{i(meas)}^g]$. The fraction (F) of gas stripping per degassing step (for a given species ‘i’) is identical in open and closed system models (see Eq. 16). However, in the closed system model the measured gas concentration $[C_{i(meas)}^g]$ at degassing step ‘d’ (instantaneous signature) is taken to represent an admixture of all previous steps (accumulated signature). In this way, gas concentrations in a closed system can be determined using a mass balance approach, following the equation:

$$[C_{i(meas)}^g] = \frac{([n_i^{asw}] - [n_i^{asw}]F^d)22400}{ZGd} \quad (13)$$

If we rearrange and simplify the equation by defining ‘U’ as:

$$U = \frac{[C_{i(meas)}^g]ZG}{22400[n_i^{asw}]} \quad (14)$$

We are then left with an equation in which ‘d’ is simultaneously in the exponential and product form:

$$Ud = 1 - F^d \quad (15)$$

This equation can then be solved for ‘d’ using a Lambert transcendental function (ω), which is defined as the multivalued inverse of the $w \rightarrow we^w$ (Corless et al., 1996)

$$d = \frac{1}{U} - \frac{1}{\ln(F)} \omega(F^{\frac{1}{U}} \ln(F)/U) \quad (16)$$

The volumetric $\frac{V_g}{V_w}$ (**SO Closed**) can be calculated by combining the d value calculated in eq. 16 with the assumed G and W volume values:

$$\frac{V_g}{V_w} (\text{SO Closed}) = \frac{dG}{W} \quad (17)$$

Using sample B-06 we calculate a $\frac{V_g}{V_w}$ (**SO Closed ²⁰Ne**) = 0.071. Notably, closed system $\frac{V_g}{V_w}$ (**SO Closed ²⁰Ne**) estimates return identical values to the (ZO) total gas stripping model, as after a modest amount of gas stripping (i.e., d steps), nearly all noble gases effectively partition into the gas phase (particularly the less soluble light noble gases). However, if the heavier noble gases are used (e.g., ³⁶Ar, ⁸⁴Kr, ¹³²Xe), then the closed system model predicts slightly lower $\frac{V_g}{V_w}$ values (Table 5) due to progressively lower partition coefficients with increasing mass. For partially

degassed closed system reservoirs this model can be used to calculate $\frac{V_g}{V_w}$ (SO Closed) at any point as degassing in a closed system proceeds.

Closed system elemental ratio volumetric $\frac{V_g}{V_w}$ (SO Closed Elemental Ratio) estimates

In a traditional closed system model (e.g., Ballentine et al., 2001), the initial “first bubble” extremum elemental ratio (i/j) is identical to an open system (eq. 10). However, the final extremum value (i.e., $\frac{V_g}{V_w} \rightarrow \infty$) is equal to the starting composition of ASW groundwater:

$$(i/j)^{final} = (i/j)_{asw} \quad (18)$$

When calculating $\frac{V_g}{V_w}$ (SO Closed Elemental Ratio) using elemental ratios in a closed system it is important to consider the evolution of the hydrocarbon system as it progresses from initial production (i.e., first bubble starting value) with very small $\frac{V_g}{V_w}$ (eq. 11) towards an ASW value with a $\frac{V_g}{V_w} > 0.01$ (Figure 7). If the elemental ratio falls between these two values then $\frac{V_g}{V_w}$ can be calculated using the following equation:

$$\frac{V_g}{V_w} (\text{SO Closed Elemental Ratio}) = \frac{\left[\frac{(i/j)_{asw}}{K_j^M} \right] - \left[\frac{(i/j)_{meas}}{K_i^M} \right]}{(i/j)_{meas} - (i/j)_{asw}} \quad (19)$$

However, this approach has a clear limitation, as once a substantial amount of the noble gases have been stripped from the initial water volume ($\frac{V_g}{V_w} > 0.01$), the elemental ratio in the gas phase approaches the ASW value (Figure 8a), and this method of estimating $\frac{V_g}{V_w}$ loses sensitivity and is rendered ineffective. If values below ASW-like values are measured (i.e., as in sample B-06), it strongly suggests open-system behaviour. Importantly, elemental ratios reveal process (i.e., open vs. closed), whereas concentration estimates remain a more accurate method (see above models) to estimate the extent of gas-water exchange and thus provide more accurate $\frac{V_g}{V_w}$ estimates as concentrations are continually diluted due to additional gas charges. For this reason a combined elemental ratio and absolute concentration approach is particularly advantageous, as the most robust $\frac{V_g}{V_w}$ estimates can be made using a combined approach providing both process and quantitation.

5.2.7 Noble Gas and Geologic $\frac{V_g}{V_w}$ Estimate Comparisons

Noble gas $\frac{V_g}{V_w}$ estimates for the four models range from 0.02-0.07. This is 3-10 times lower than the geological estimate of ~0.24. The elemental ratios (e.g., $^{20}\text{Ne}/^{36}\text{Ar}$) reveal that the system must be open (Figure 8a), as it is the only viable mechanism to reach the observed values. This is entirely consistent with our geological understanding of this field. The gases in the Sleipner Ost field are thought to have migrated through Sleipner Vest, which itself has been filled to spill. The extent of exchange (and thus the $\frac{V_g}{V_w}$) cannot be accurately assessed using elemental ratios alone and therefore concentrations are used in addition to elemental ratios to calculate $\frac{V_g}{V_w}$. In this way, we calculate a $\frac{V_g}{V_w}$ (**OS ^{20}Ne**) value of ~0.019 (Table 5) that we view as the most robust estimate possible using sample B-06. If sample B-06 is actually slightly contaminated, requiring further correction to infer the true Sleipner reservoir composition, then an extrapolation along an air-mixing line through all data intersects the open system line yielding an estimate for $\frac{V_g}{V_w}$ of ~0.022. This extrapolation does not return a significantly different solution and the result is still an order of magnitude lower than static geological $\frac{V_g}{V_w}$ estimates. The extent of gas loss in an open system can be quantified in terms of the total number of reservoir volumes that have passed through the system. For the two scenarios above we estimate that between 8 to 10 reservoir volumes must have been lost to a fill and spill, based on the Ne concentration.

The implications for lower noble gas $\frac{V_g}{V_w}$ from noble gas estimates vs. static geological estimates are two-fold: 1) the Sleipner Vest system either has a dynamically flowing aquifer system and/or 2) it has experienced significant gas-water exchange along its migration pathway not accounted for in the geologic estimates. The latter interpretation is preferred and implies that noble gas exchange during migration could be the dominant process controlling noble gas distributions in Sleipner Vest. It is worth noting here that the “geological” estimate of gas-water volumetric ratios only consider gas and water volumes in the Hugin reservoir. It does not therefore consider any water or gas present in deeper structures, the migration pathway or the source rock. In this context, the noble gases provide constraints on all formation water encountered in the hydrocarbon system, not only the reservoir interval. It is therefore not surprising that noble gas estimates of formation water exceed those from static geological estimates. Similarly, it is widely known that Sleipner gases migrate through reservoir intervals in deeper sections of the South Viking Graben as depicted in Fig. 2. This is again consistent with the larger volumes of water (smaller gas/water ratios) that our noble gas models predict compared to the static geological estimates.

The highest $\frac{V_g}{V_w}$ estimates are from Ne-Ar constraints; if Ne-Ar models are considered most robust for predicting $\frac{V_g}{V_w}$, due to their relatively low solubility in fluids, then the Kr-Xe values are likely in excess and thus underestimate $\frac{V_g}{V_w}$ ratios. This conclusion is supported by large heavy noble gas enrichments relative to predicted Ne depletions in an open system (Figure 6c). It also suggests that an additional source of heavy noble gases other than ASW is present in Sleipner Vest gases. The sources of these excesses are discussed in section 5.4.

5.3 Additional Controls on noble gas models

There are a number of factors that can modify measured noble gases in hydrocarbons including: secondary air contamination, variable recharge, source and storage conditions, migration history, hydrocarbon phase (oil vs. gas), and secondary fluid-rock exchange. These processes can be identified and constrained by investigating noble gas elemental patterns and measurements of all air-derived noble gases, together with radiogenic-derived noble gases.

5.3.1 Interaction with extraneous air

Small additions of extraneous air acquired during the sampling procedure can potentially skew noble gas data significantly. In Figure 7, $^{20}\text{Ne}/^{36}\text{Ar}$ is plotted as a function of Ne concentration (in the gas phase), along with predicted (open and closed system) gas-stripping trajectories. Any secondary/extraneous addition of air falls on a distinct trend away from these degassing trends (Figure 7). Sample B-06 is taken as the starting point by which the mixing trajectory between closed system evolution and any secondary air contributions is plotted, due to the fact that it is the least contaminated sample. The remaining 'Normal Samples' from Sleipner can be explained by very small (0.03-0.05%) amounts of air contamination. In contrast, the (n=3) 'outlier samples' require between 1.0-1.2% air contamination to explain their coupled Ne-Ar characteristics in Figure 7. This data set highlights the sensitivity of noble gases to small amounts of air-contamination. However, by identifying the least contaminated sample (B-06), we are still able to make an estimation of $\frac{V_g}{V_w}$ despite the fact that there is small but pervasive air contamination in most samples.

5.3.2 Hybrid models

There are a number of possible hybrid scenarios whereby the hydrocarbon system undergoes multiple stages of open and closed system evolution. For example, the system can initially be open, and then becomes closed. Alternatively, the system could initially be closed and then become open. These scenarios are depicted graphically in Figures 9a-b. For example, Figure 9a depicts a simple closed-system scenario whereby hydrocarbon gases migrate from a graben at depth, and are stored in a reservoir where there is no gas escape. Variations of this scenario are described in sections 5.2 (i.e., ZO – total gas stripping; FO – equilibrium degassing; SO – closed-system concentrations and elemental ratios). Figure 9b depicts a fill and spill scenario that is initially identical to the closed system evolution depicted in Figure 9a, which then becomes open once the reservoir is filled. In this scenario,

degassing trajectories would first follow the shape of a closed system and later diverge to an open system trajectory, with more extensive fractionation.

5.4 Heavy noble gas enrichments

There are clear excesses of heavy noble gases relative to what is predicted based on ASW and solubility constraints (Table 2). As a result, solubility models are unable to predict a realistic volumetric gas-water ratios (Table 5). In this section we explore potential reasons for inconsistencies between heavy noble gas predictions and observations. In Figure 6 we plot $(\text{noble gas } i / ^{36}\text{Ar})_{\text{sample}} / (\text{noble gas } i / ^{36}\text{Ar})_{\text{ASW}}$, where noble gas i is an air derived noble gas (i.e., ^{20}Ne , ^{36}Ar , ^{84}Kr and ^{132}Xe). By definition ASW is therefore equal to unity. Notably, $^{20}\text{Ne}/^{36}\text{Ar}$ for sample B-06 plots below the ASW line and $^{84}\text{Kr}/^{36}\text{Ar}$ and $^{132}\text{Xe}/^{36}\text{Ar}$ ratios plot above the ASW line, suggesting open system behavior (Figure 6c). Due to this enrichment, heavy noble gas $\frac{V_g}{V_w}$ estimates are consistently lower, suggesting that they may have an additional source of Kr and Xe in the crust. In organic-rich sedimentary lithologies (e.g., shales and cherts), the heavier noble gas species (Kr-Xe) have been shown to preferentially absorb onto minerals (Podosek et al., 1981). If these noble gas laden lithologies are buried to depths sufficient for the generation of hydrocarbons, the resultant hydrocarbons will have marked heavy noble gas enrichments due to desorption at such temperatures. As a result, high relative abundances of Xe and Kr relative to light noble gases (Figure 6c) will be imparted upon samples (Hiyagon and Kennedy, 1992; Torgersen and Kennedy, 1999; Zhou et al., 2005). Any ensuing mixing with ASW-derived noble gases will result in dilution of the trapped component signal, which can be observed by decreasing $^{132}\text{Xe}/^{36}\text{Ar}$ values.

In sample B-06 the heavy/light elemental ratios show a marked increase compared to predicted groundwater values; i.e., B-06 has a $^{20}\text{Ne}/^{36}\text{Ar}$ value slightly below ASW, and higher $^{132}\text{Xe}/^{36}\text{Ar}$, $^{84}\text{Kr}/^{36}\text{Ar}$ ratios than that predicted for a closed system solubility relationship. Figure 6c shows clear relative enrichments in heavy noble gases from Sleipner Vest. Previous studies have shown similar heavy noble gas enrichments; for example Torgersen and Kennedy, 1999 reported $(^{132}\text{Xe}/^{36}\text{Ar})_{\text{Meas.}} / (^{132}\text{Xe}/^{36}\text{Ar})_{\text{Air}}$ up to 576 in gases separated from oil-associated gases from the Elk Hills oil fields, California. Similarly, Zhou et al., 2005 reported $(^{132}\text{Xe}/^{36}\text{Ar})_{\text{Meas.}} / (^{132}\text{Xe}/^{36}\text{Ar})_{\text{Air}}$ of approximately 100 in coal bed gases from the San Juan Basin.

Gas-oil interaction can potentially result in heavy noble gas enrichments (Kharaka and Spect, 1988; Bosch and Mazor, 1988). The effect of oil would be similar to having a very saline starting reservoir, in that it would strip away the initial noble gas inventory and fractionate elemental ratios. The direction of fractionation of the light elemental ratios ($^{20}\text{Ne}/^{36}\text{Ar}$) suggests that groundwater-derived noble gases in the Sleipner Vest natural gas samples have experienced extensive gas/water phase partitioning (approaching total gas stripping). However, an open system Rayleigh fractionation process, where small amounts of gas continually exsolve from the groundwater

and are removed from the system is more difficult to reconcile with the heavy noble gas data. Indeed, elemental fractionation patterns are much more extreme (Figure 6c) and seemingly at odds with measured concentrations, which suggest less degassing or, alternatively, heavy noble gas enrichments from a secondary source (Figure 6c). For reference we also plot air, however such enrichments in Kr-Xe are in the opposite direction as would be anticipated based on interaction with air.

5.5 Radiogenic noble gases

Helium isotopes suggest that Sleipner Vest gases are strongly radiogenic, with He-isotope values ranging from 0.065-0.116 R_A . If we assume binary mixing between crustal and mantle endmembers of 0.007 R_A and 6.1 R_A (Zhou et al., 2006; Day et al., 2015), respectively, then we calculate a crustal contribution between 98.2 to 99.0%. This suggests that mantle contributions to the system are on the order of 1%, and thus negligible for the purpose of modelling. Therefore, any excess ^4He can be attributed to radiogenic ingrowth. Radiogenic noble gas nuclides (e.g., ^4He) are produced in crustal rocks by the radiogenic decay of parent nuclides (e.g., U-Th), and are subsequently transferred into the surrounding groundwater. The extent of transfer is a function of parent nuclide abundance in the source mineral, as well as reservoir conditions (e.g., temperature, thickness and porosity). The concentration of radiogenic noble gases within hydrocarbon reservoirs is controlled by the extent of hydrocarbon interaction with groundwater and the open or closed nature of the exchange (see Section 5.2). Furthermore, mechanical shear within the aquifer releases He that accumulated over long durations in minerals, but is only loosely bound. Under such conditions radiogenic He is related to mechanical friction and in turn radiogenic ages should only be treated as a semi-quantitative estimate (e.g., Aeschbach-Hertig and Solomon, 2013).

Noble gas partitioning models suggest that Sleipner Vest is an open system (based on ^{20}Ne and ^{36}Ar compositions), and that approximately 8-10 reservoir volumes have 'filled and spilled' through the system. By assuming 1) both groundwater-derived noble gases (e.g., ^{20}Ne and ^{36}Ar) and crustal radiogenic noble gases (e.g. ^4He) are coherently fractionated according to known relative partitioning behaviour (i.e., K_i/K_j), irrespective of their source, 2) 'in-situ reservoir' and 'source rock derived' radiogenic contributions are negligible relative to those acquired through hydrocarbon-groundwater exchange and 3) Sleipner Vest is indeed an open system (8-10 reservoir volumes have been lost), then the measured concentration of radiogenic ^4He in the gas phase of sample B-06 ($5.8 \times 10^{-5} \text{ cm}^3 \text{ STP } ^4\text{He}$) can be used to estimate the initial concentration of ^4He in the groundwater ($1.1 \times 10^{-3} \text{ cm}^3 \text{ STP } ^4\text{He} / \text{cm}^3 \text{ H}_2\text{O}$). This initial concentration represents the amount that is required to have originally been in the water that was subsequently stripped of its noble gases, to form the Sleipner Vest gas reservoir. The estimated concentration in the initial water can then be combined with a predicted helium flux from the reservoir. In-situ radiogenic ingrowth has previously been shown to be negligible in conventional hydrocarbon reservoirs (e.g., Elliot et al., 1993; Ballentine et al., 1996; Ballentine and Sherwood-Lollar, 2002; Zhou and Ballentine, 2006), and thus we

only consider an external ^4He ingrowth, which assumes a steady state ^4He flux, proposed by Torgersen and Ivey, 1985. Using the methods of Zhou and Ballentine, 2006, we calculate an external ^4He accumulation rate of $9.24 \times 10^{-10} \text{ cm}^3 \text{ STP } ^4\text{He} / \text{cm}^3 \text{ H}_2\text{O} \text{ year}$ for the Sleipner Vest reservoir; we assume an average total crustal ^4He flux of $2.31 \times 10^6 \text{ cm}^3 \text{ STP } ^4\text{He} / \text{cm}^2 \text{ year}$ (Taylor and McLennan, 1985), and the same porosity (18%) and an average reservoir thickness (150m) for the Hugin Sandstone (Folkestad and Satur, 2008) as was used in making static gas-water estimates (Section 5.2.1). When this ^4He accumulation rate is combined with the initial concentration estimate of radiogenic ^4He in the formation water (B-06 = $1.1 \times 10^{-3} \text{ cm}^3 \text{ STP } ^4\text{He} / \text{cm}^3 \text{ H}_2\text{O}$), it yields an age for the aquifer water of approximately 1.3 Ma. If we assume that the radiogenic inventory was acquired over a longer timescale and prior to hydrocarbon production, then this estimate puts constraints on the time scale for hydrocarbon production, secondary migration and trapping processes. The observation that $^4\text{He}/^{40}\text{Ar}^*$ ($^{40}\text{Ar}^* = \text{air corrected radiogenic Ar}$) values (Figure 5d) span a limited range (4.9-6.5), confirms that radiogenic ingrowth must have occurred prior to emplacement of the hydrocarbon phase in the reservoir. We suggest that radiogenic components were homogenized in the groundwater, prior to gas stripping due to interaction with hydrocarbons. The consistency in $^4\text{He}/^{40}\text{Ar}^*$ also confirms that samples have been uniformly affected by partitioning, which lends further credence to using B-06 to characterize the Sleipner Vest system.

6. Summary

In this contribution we present compositional, stable isotope and noble gas isotope and abundance data from the Sleipner Vest field, in the Norwegian North Sea. Noble gases are predominantly crustal and ASW-derived, with negligible mantle contributions. These data are discussed within the framework of four conceptual models: i) Total gas-stripping model, which defines the minimum volume of water to have interacted with the hydrocarbon phase; ii) Equilibrium model, assuming simple equilibration between groundwater and hydrocarbon phase at reservoir P, T and salinity; iii) Open system gas-stripping and iv) Closed system gas-stripping models. Using Ne-Ar, we estimate gas-water ratios for the Sleipner system of 0.02-0.07, with a best estimate of ~ 0.02 . The most confidence is given to open system Ne-Ar estimates, which are approximately an order of magnitude lower than static geologic gas-water estimates of ~ 0.24 . Noble-gas-based $\frac{V_g}{V_w}$ estimates suggest more groundwater interaction than a static system estimate, which can be attributed to a dynamically flowing aquifer system and/or a hydrous hydrocarbon migration pathway. Assuming that the Sleipner Vest system is in fact an open system, we estimate that between 8-10 reservoir volumes of gas have been filled and spilled from the current system, to result in the observed Ne-Ar systematics. This estimate can be used to place constraints on the overall timing of hydrocarbon-water exchange. If we assume that the radiogenic inventory was acquired prior to hydrocarbon production, and a steady-state ^4He flux, we calculate that hydrocarbon production, secondary migration and trapping processes occurred over approximately 1.3 Ma.

668

669 **Acknowledgments**

670 We acknowledge ExxonMobil for funding this research and ExxonMobil and their subsidiaries for providing
671 samples. We thank Michael Broadley for extensive discussions, which helped advance many of the ideas presented
672 here. We thank Diveena Danabalan for analytical assistance and discussions. We thank Dave Sansom for assistance
673 with making figures. We acknowledge Tom Darrah and two anonymous reviewers for their constructive and
674 helpful reviews, as well as Chris Hall for editorial handling.

675

676 **References**

677 Aeschbach-Hertig, W., & Solomon, D. K. (2013). Noble gas thermometry in groundwater hydrology. In *The*
678 *noble gases as geochemical tracers* (pp. 81-122). Springer Berlin Heidelberg.

679 Aregbe, Y., Valkiers, S., Mayer, K., & De Bièvre, P. (1996). Comparative isotopic measurements on xenon
680 and krypton. *International journal of mass spectrometry and ion processes*, 153(1), L1-L5.

681 Barry, P. H., Hilton, D. R., Day, J. M., Pernet-Fisher, J. F., Howarth, G. H., Magna, T., Agashev, A.M.,
682 Pokhilenko, N.P., Pokhilenko, L.N. & Taylor, L. A. (2015). Helium isotopic evidence for modification of the cratonic
683 lithosphere during the Permo-Triassic Siberian flood basalt event. *Lithos*, 216, 73-80.

684 Ballentine, C. J., O'nions, R. K., Oxburgh, E. R., Horvath, F., & Deak, J. (1991). Rare gas constraints on
685 hydrocarbon accumulation, crustal degassing and groundwater flow in the Pannonian Basin. *Earth and Planetary*
686 *Science Letters*, 105(1), 229-246.

687 Ballentine, C. J., O'Nions, R. K., & Coleman, M. L. (1996). A Magnus opus: Helium, neon, and argon
688 isotopes in a North Sea oilfield. *Geochimica et Cosmochimica Acta*, 60(5), 831-849.

689 Ballentine, C. J., & Burnard, P. G. (2002). Production, release and transport of noble gases in the
690 continental crust. *Reviews in mineralogy and geochemistry*, 47(1), 481-538.

691 Ballentine, C. J., & Lollar, B. S. (2002). Regional groundwater focusing of nitrogen and noble gases into the
692 Hugoton-Panhandle giant gas field, USA. *Geochimica et Cosmochimica Acta*, 66(14), 2483-2497.

693 Bosch, A., & Mazor, E. (1988). Natural gas association with water and oil as depicted by atmospheric noble
694 gases: case studies from the southeastern Mediterranean Coastal Plain. *Earth and planetary science letters*, 87(3),
695 338-346.

696 Burnard, P. (2013). The Noble Gases as Geochemical Tracers. Springer.

697 Castro, M. C., Jambon, A., Marsily, G., & Schlosser, P. (1998a). Noble gases as natural tracers of water
698 circulation in the Paris Basin: 1. Measurements and discussion of their origin and mechanisms of vertical transport
699 in the basin. *Water Resources Research*, 34(10), 2443-2466.

700 Castro, M. C., Goblet, P., Ledoux, E., Violette, S., & de Marsily, G. (1998b). Noble gases as natural tracers
701 of water circulation in the Paris Basin. 2. Calibration of a groundwater flow model using noble gas isotope data.
702 *Water Resources Research*, 34(10), 2467-2483.

703 Clarke, W. B., Jenkins, W. J., & Top, Z. (1976). Determination of tritium by mass spectrometric
704 measurement of 3 He . *The international journal of applied radiation and isotopes*, 27(9), 515-522.

705 Cook, P. G., Solomon, D. K., Sanford, W. E., Busenberg, E., Plummer, L. N., & Poreda, R. J. (1996). Inferring
706 shallow groundwater flow in saprolite and fractured rock using environmental tracers. *Water Resources Research*,
707 32(6), 1501-1509.

708 Corless, R. M., Gonnet, G. H., Hare, D. E., Jeffrey, D. J., & Knuth, D. E. (1996). On the LambertW function.
709 *Advances in Computational mathematics*, 5(1), 329-359.

710 Crovetto, R., Fernández-Prini, R., Japas, M.L., 1982. Solubilities of inert gases and methane in H_2O and in
711 D_2O in the temperature range of 300 to 600 K. *The Journal of Chemical Physics* 76, 1077–1086.
712 doi:10.1063/1.443074.

713 Darrah, T. H., Vengosh, A., Jackson, R. B., Warner, N. R., & Poreda, R. J. (2014). Noble gases identify the
714 mechanisms of fugitive gas contamination in drinking-water wells overlying the Marcellus and Barnett Shales.
715 *Proceedings of the National Academy of Sciences*, 111(39), 14076-14081.

716 Darrah, T.H., Jackson, R.B., Vengosh, A., Warner, N.R., Whyte, C.J., Walsh, T.B., Kondash, A.J. & Poreda,
717 R.J., (2015). The evolution of Devonian hydrocarbon gases in shallow aquifers of the northern Appalachian Basin:
718 Insights from integrating noble gas and hydrocarbon geochemistry. *Geochimica et Cosmochimica Acta*, 170,
719 pp.321-355.

720 Day, J. M., Barry, P. H., Hilton, D. R., Burgess, R., Pearson, D. G., & Taylor, L. A. (2015). The helium flux
721 from the continents and ubiquity of low- $3\text{ He}/4\text{ He}$ recycled crust and lithosphere. *Geochimica et Cosmochimica*
722 *Acta*, 153, 116-133.

723 Elliot, T., Ballentine, C. J., O'nions, R. K., & Ricchiuto, T. (1993). Carbon, helium, neon and argon isotopes in
724 a Po Basin (northern Italy) natural gas field. *Chemical Geology*, 106(3), 429-440.

725 Folkestad, A., & Satur, N. (2008). Regressive and transgressive cycles in a rift-basin: Depositional model
726 and sedimentary partitioning of the Middle Jurassic Hugin Formation, Southern Viking Graben, North Sea.
727 *Sedimentary Geology*, 207(1), 1-21.

728 Gilfillan, S. M., Ballentine, C. J., Holland, G., Blagburn, D., Lollar, B. S., Stevens, S., Schoell, M. & Cassidy, M.
729 (2008). The noble gas geochemistry of natural CO₂ gas reservoirs from the Colorado Plateau and Rocky Mountain
730 provinces, USA. *Geochimica et Cosmochimica Acta*, 72(4), 1174-1198.

731 Gilfillan, S. M., Lollar, B. S., Holland, G., Blagburn, D., Stevens, S., Schoell, M., Cassidy, M., Ding, Z., Zhou,
732 Z., Lacrampe-Couloume, G. & Ballentine, C. J. (2009). Solubility trapping in formation water as dominant CO₂ sink
733 in natural gas fields. *Nature*, 458(7238), 614-618.

734 Harris, J.P., and Fowler, R.M., 1987, Enhanced prospectivity of the Mid-Late Jurassic sediments of the
735 South Viking Graben, northern North Sea, in J. Brooks and K. Glennie, eds., *Petroleum geology of north-west*
736 *Europe*, Graham and Trotman, London, p. 879-898. Hiyagon, H., & Kennedy, B. M. (1992). Noble gases in CH₄-rich
737 gas fields, Alberta, Canada. *Geochimica et Cosmochimica Acta*, 56(4), 1569-1589. Pinti and Marty, 1995;

738 Husmo, T., Hamar, G.P., Høiland, O., Johanessen, E.P., Rømuld, A., Spencer, A.M., and Titterton, R., 2003,
739 Lower and Middle Jurassic, in Evans, D., Graham, C., Armour, A., and Bathurst, P., eds., *The Millennium Atlas:*
740 *petroleum geology of the central and northern North Sea*: Geological Society, London, p. 129-155.

741 Hunt, A. G., Darrah, T. H., & Poreda, R. J. (2012). Determining the source and genetic fingerprint of natural
742 gases using noble gas geochemistry: A northern Appalachian Basin case study. *Aapg Bulletin*, 96(10), 1785-1811.

743 Isaksen, G.H., Patience, R., van Graas, G., Jenssen, A.I. (2002) Hydrocarbon system analysis in a rift basin
744 with mixed marine and nonmarine source rocks: The South Viking Graben, North Sea. *AAPG Bulletin*, 86, 557-591.

745 Lee, J. Y., Marti, K., Severinghaus, J. P., Kawamura, K., Yoo, H. S., Lee, J. B., & Kim, J. S. (2006). A
746 redetermination of the isotopic abundances of atmospheric Ar. *Geochimica et Cosmochimica Acta*, 70(17), 4507-
747 4512.

748 Lowenstern, J. B., Evans, W. C., Bergfeld, D., & Hunt, A. G. (2014). Prodigious degassing of a billion years of
749 accumulated radiogenic helium at Yellowstone. *Nature*, 506(7488), 355-358.

750 Niedermann, S., Graf, T., & Marti, K. (1993). Mass spectrometric identification of cosmic-ray-produced
751 neon in terrestrial rocks with multiple neon components. *Earth and Planetary Science Letters*, 118(1), 65-73.

752 Ostvedt, O. J., Evensen, S., & Ranaweera, H. K. A. (1990). Sleipner Ost Field--Norway Viking Graben, North
753 Sea.

754 Pepin, R. O. (2000). On the isotopic composition of primordial xenon in terrestrial planet atmospheres. In
755 From Dust to Terrestrial Planets (pp. 371-395). Springer Netherlands.

756 Pinti, D. L., & Marty, B. (1995). Noble gases in crude oils from the Paris Basin, France: Implications for the
757 origin of fluids and constraints on oil-water-gas interactions. *Geochimica et Cosmochimica Acta*, 59(16), 3389-
758 3404.

759 Podosek, F. A., Bernatowicz, T. J., & Kramer, F. E. (1981). Adsorption of xenon and krypton on shales.
760 *Geochimica et Cosmochimica Acta*, 45(12), 2401-2415.

761 Prinzhofer, A. (2013). Noble Gases in Oil and Gas Accumulations. In *The Noble Gases as Geochemical*
762 *Tracers* (pp. 225-247). Springer Berlin Heidelberg.

763 Sano, Y., Wakita, H., & Sheng, X. (1988). Atmospheric helium isotope ratio. *Geochemical Journal*, 22(4),
764 177-181.

765 Schwarzenbach, R. S., P. M. Gschwend, & D. M. Imboden (2003). *Environmental Organic Chemistry*, 2nd
766 ed., John Wiley, Hoboken, N. J.

767 Smith, S.P., Kennedy, B.M., 1983. The solubility of noble gases in water and in NaCl brine. *Geochimica et*
768 *Cosmochimica Acta* 47, 503–515. doi:10.1016/0016-7037(83)90273-9

769 Smith, S. P. (1985). Noble gas solubility in water at high temperature. *Eos*, 66, 397.

770 Solomon, D. K., Hunt, A., & Poreda, R. J. (1996). Source of radiogenic helium 4 in shallow aquifers:
771 Implications for dating young groundwater. *Water Resources Research*, 32(6), 1805-1813.

772 Stolper, D. A., Lawson, M., Davis, C. L., Ferreira, A. A., Neto, E. S., Ellis, G. S., Lewan, M.D., Martini, A.M.,
773 Tang, Y., Shoell, M., Sessions, A.L., & Eiler, J. M. (2014). Formation temperatures of thermogenic and biogenic
774 methane. *Science*, 344(6191), 1500-1503.

775 Taylor, S. R., & McLennan, S. M. (1985). The continental crust: its composition and evolution.

776 Torgersen, T., & Clarke, W. B. (1985). Helium accumulation in groundwater, I: An evaluation of sources
777 and the continental flux of crustal 4 He in the Great Artesian Basin, Australia. *Geochimica et Cosmochimica Acta*,
778 49(5), 1211-1218.

779 Torgersen, T., & Ivey, G. N. (1985). Helium accumulation in groundwater. II: A model for the accumulation
780 of the crustal 4 He degassing flux. *Geochimica et Cosmochimica Acta*, 49(11), 2445-2452.

781 Torgersen, T., & Kennedy, B. M. (1999). Air-Xe enrichments in Elk Hills oil field gases: role of water in
782 migration and storage. *Earth and Planetary Science Letters*, 167(3), 239-253.

783 Torgersen, T. (2010). Continental degassing flux of 4He and its variability. *Geochemistry, Geophysics,*
784 *Geosystems*, 11(6).

785 Tolstikhin, I., Kamensky, I., Tarakanov, S., Kramers, J., Pekala, M., Skiba, V., Gannibal, M., & Novikov, D.
786 (2010). Noble gas isotope sites and mobility in mafic rocks and olivine. *Geochimica et Cosmochimica Acta*, 74(4),
787 1436-1447.

788 Warr, O., Rochelle, C. A., Masters, A., & Ballentine, C. J. (2015). Determining noble gas partitioning within
789 a $\text{CO}_2\text{-H}_2\text{O}$ system at elevated temperatures and pressures. *Geochimica et Cosmochimica Acta*, 159, 112-125.

790 Zaikowski, A., & Spangler, R. R. (1990). Noble gas and methane partitioning from ground water: An aid to
791 natural gas exploration and reservoir evaluation. *Geology*, 18(1), 72-74.

792 Zhou, Z., Ballentine, C. J., Kipfer, R., Schoell, M., & Thibodeaux, S. (2005). Noble gas tracing of
793 groundwater/coalbed methane interaction in the San Juan Basin, USA. *Geochimica et Cosmochimica Acta*, 69(23),
794 5413-5428.

795 Zhou, Z., & Ballentine, C. J. (2006). 4He dating of groundwater associated with hydrocarbon reservoirs.
796 *Chemical Geology*, 226(3), 309-327.

797 Zhou, Z., Ballentine, C. J., Schoell, M., & Stevens, S. H. (2012). Identifying and quantifying natural CO_2
798 sequestration processes over geological timescales: The Jackson Dome CO_2 Deposit, USA. *Geochimica et*
799 *Cosmochimica Acta*, 86, 257-275.

800 Zumberge, J., Ferworn, K., & Brown, S. (2012). Isotopic reversal ('rollover') in shale gases produced from
801 the Mississippian Barnett and Fayetteville formations. *Marine and Petroleum Geology*, 31(1), 43-52.

802 Zartman, R. E., Wasserburg, G. J., & Reynolds, J. H. (1961). Helium, argon, and carbon in some natural
803 gases. *Journal of Geophysical Research*, 66(1), 277-306.

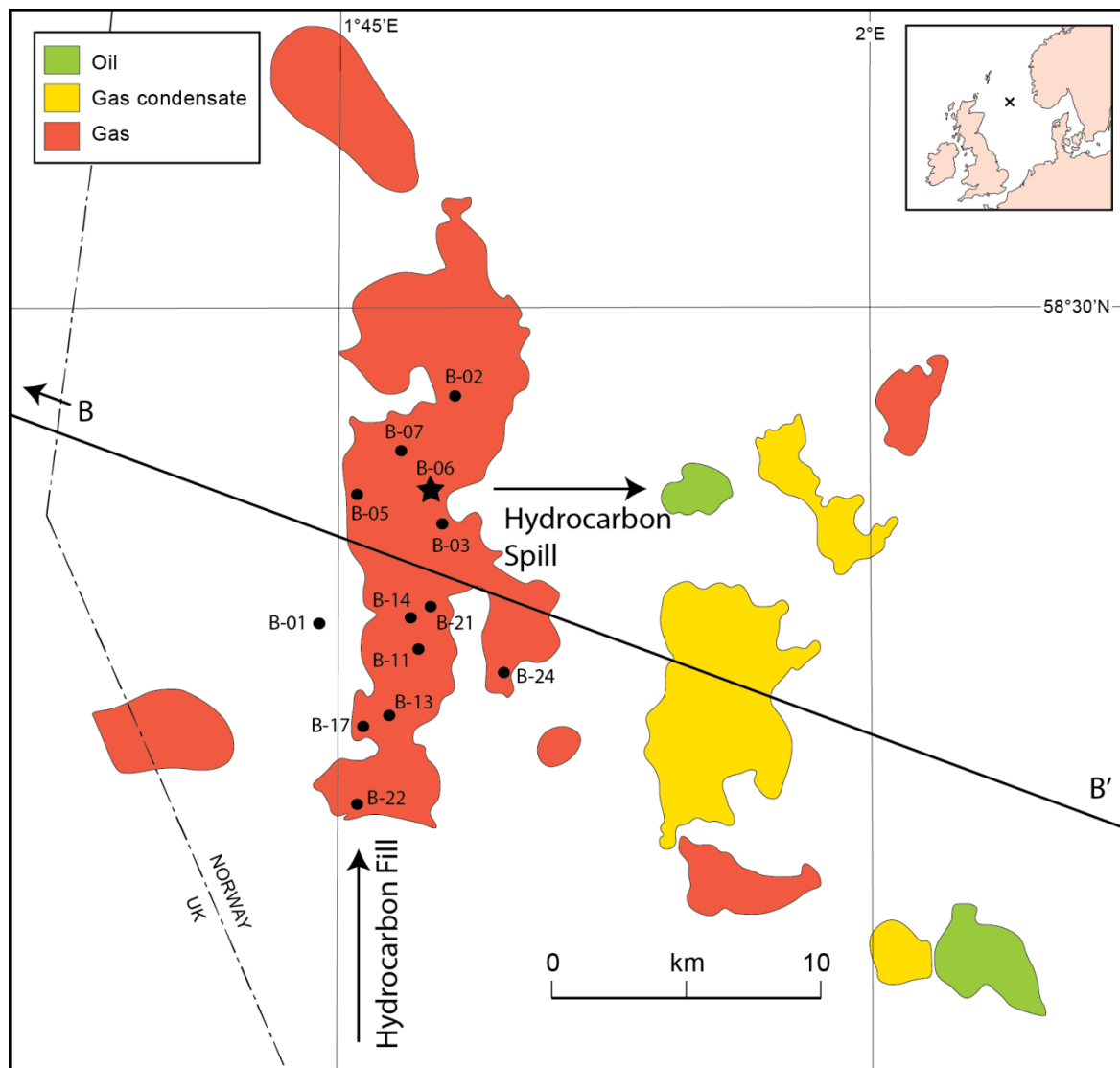


Figure 1 – Map showing the extent of oil, gas condensate and gas accumulations in the Sleipner Field. Sleipner Vest is shown in red whereas Sleipner Ost is shown in yellow. Methane gas is the dominant hydrocarbon phase found in all fields. Hydrocarbon fill is occurring from the south and spilling (into Sleipner Ost) to the east. The B-B' line shows where the cross-section (Figure 2) cuts through this segment of the field. Figure is adapted from Ostvedt et al., 1990.

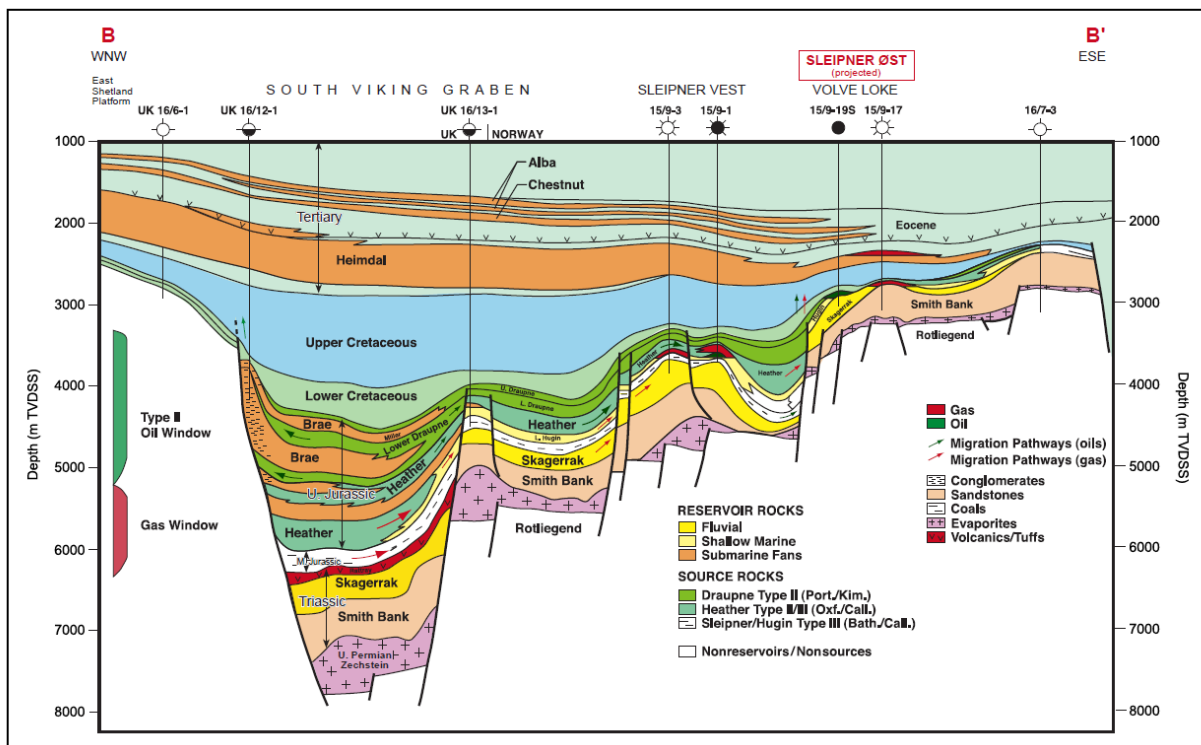


Figure 2 – Geologic cross section of the the South Viking Graben. Natural gas in this field is hosted in the dominantly lower shoreface sandstones of the Jurassic Hugin formation. The petroleum system is sealed by the Jurassic Upper Draupne and Heather formations. The likely source intervals for these hydrocarbons include the oil prone pre-upper Draupne (dominantly algal marine type II kerogen) and Heather (mixed algal marine and terrestrial type II/III kerogen) source intervals, as well as more gas prone dominantly terrestrial type III Hugin and Sleipner sources. Figure adapted from Isaksen et al., 2002.

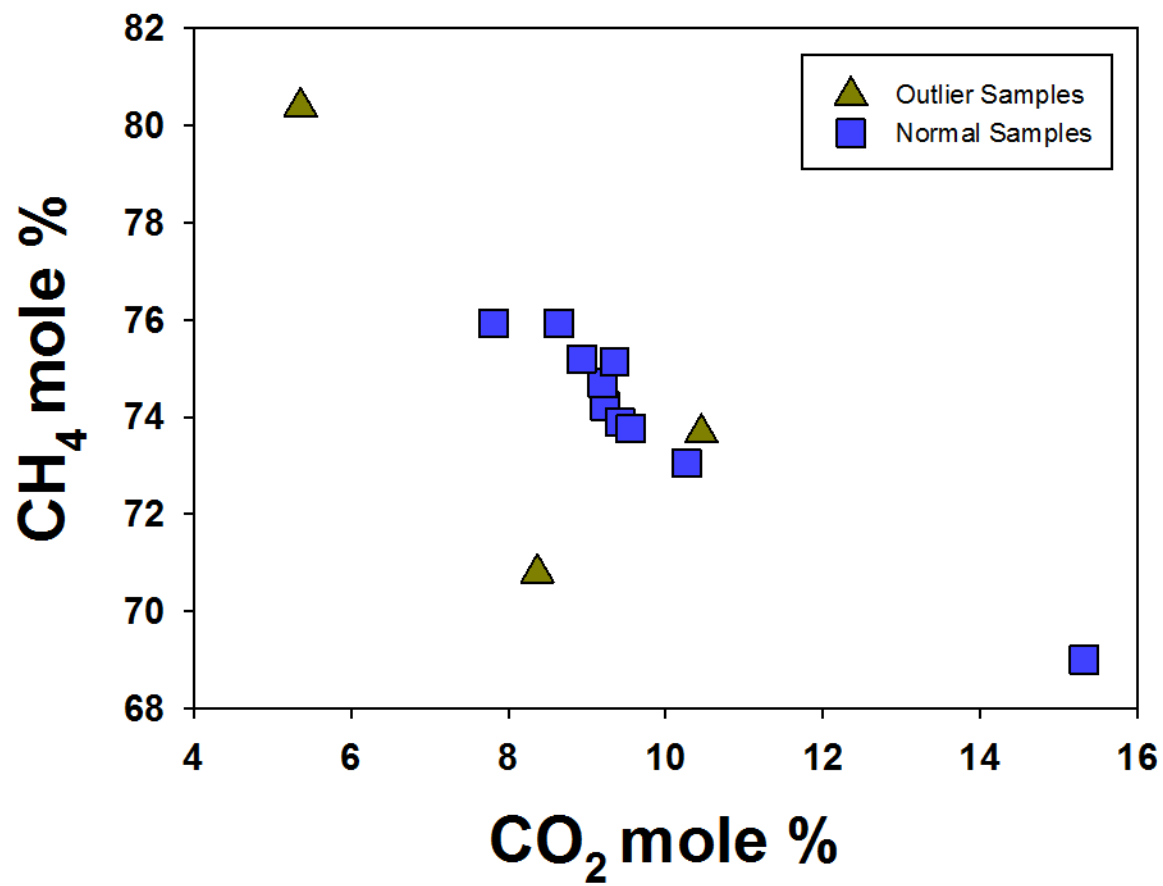


Figure 3 – CH₄ vs. CO₂ mole %, showing a strong negative correlation in normal samples ($R^2 = 0.94$). Some outlier samples fall off of this same trend.

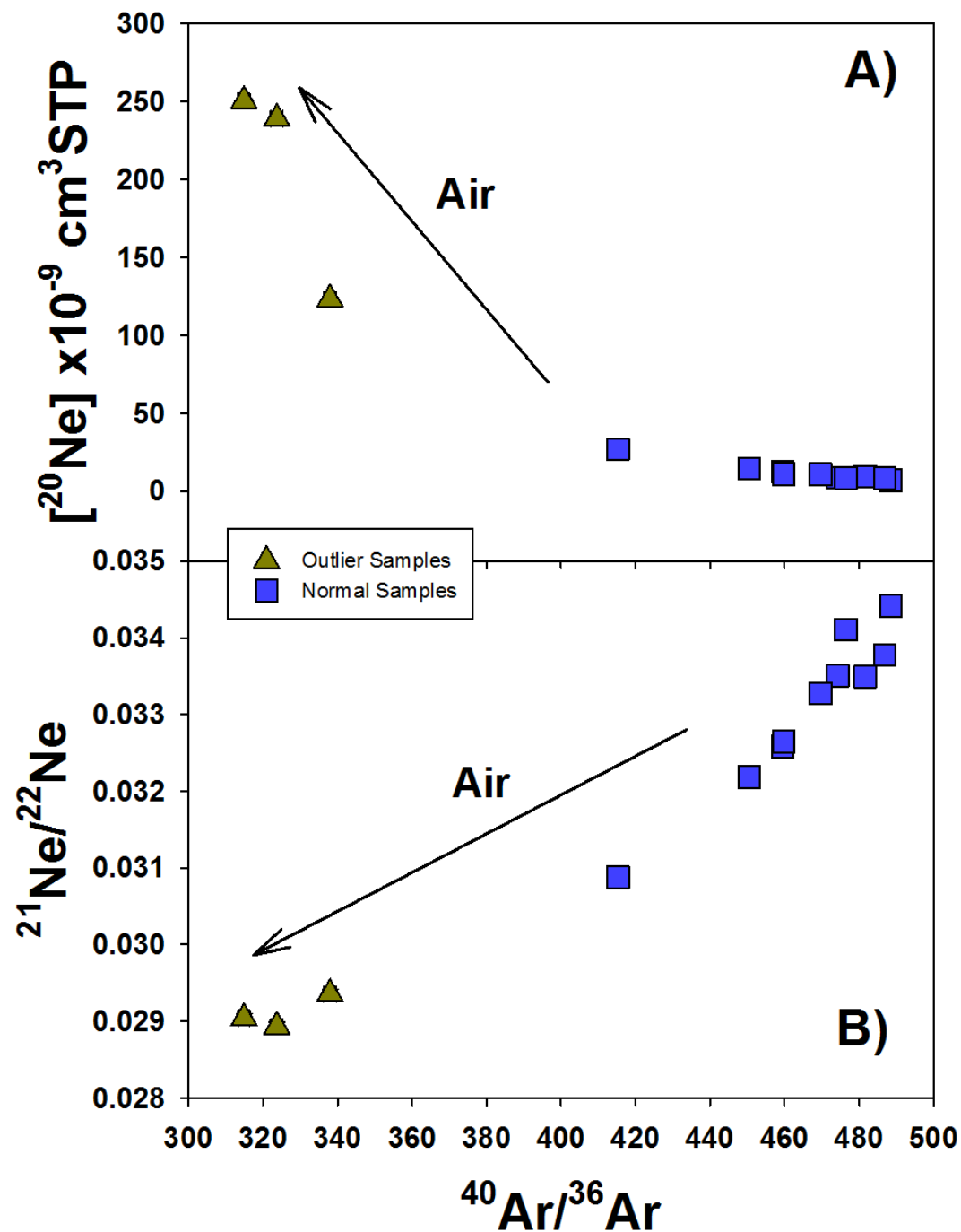


Figure 4a) – Ne concentration vs. Ar-isotopes ($^{40}\text{Ar}/^{36}\text{Ar}$) 4b) Ne-isotopes ($^{21}\text{Ne}/^{22}\text{Ne}$) vs. Ar-isotopes ($^{40}\text{Ar}/^{36}\text{Ar}$). Both figures illustrate the modifying effect of air contamination in the 'outlier samples' shown as gold triangles as opposed to the normal Sleipner vest samples, shown as blue squares.

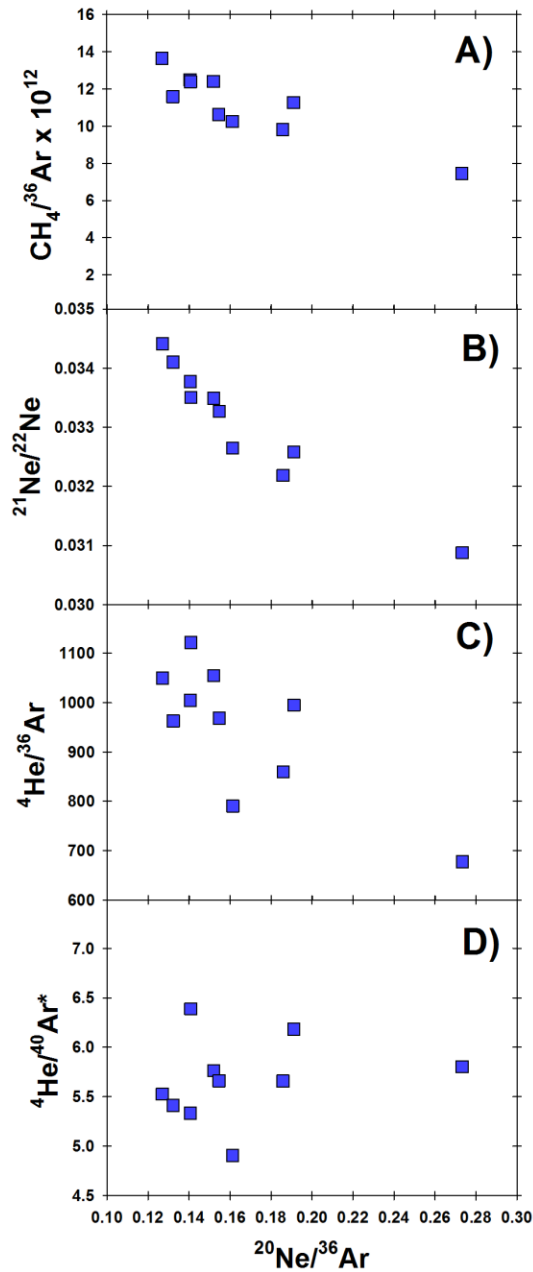


Figure 5a) – $\text{CH}_4/^{36}\text{Ar}$ vs. $^{20}\text{Ne}/^{36}\text{Ar}$, showing a strong negative correlation; 5b) – Ne-isotopes ($^{21}\text{Ne}/^{22}\text{Ne}$) vs. $^{20}\text{Ne}/^{36}\text{Ar}$ showing that the least contaminated samples display the highest Ne-isotopes and lowest $^{20}\text{Ne}/^{36}\text{Ar}$; 5c) – $^4\text{He}/^{36}\text{Ar}$ vs. $^{20}\text{Ne}/^{36}\text{Ar}$, showing a negative correlation; 5d) – Radiogenic $^4\text{He}/^{40}\text{Ar}^*$ vs. air-derived $^{20}\text{Ne}/^{36}\text{Ar}$; the fact that $^4\text{He}/^{40}\text{Ar}^*$ ($^{40}\text{Ar}^*$ = air corrected radiogenic Ar) values span such a small range suggests that radiogenic noble gases were partitioned evenly. The fact that B-06 plots intermediately in that range, indicates that B-06 is representative of the Sleipner Vest system. Note that only ‘Normal Samples’ are plotted.

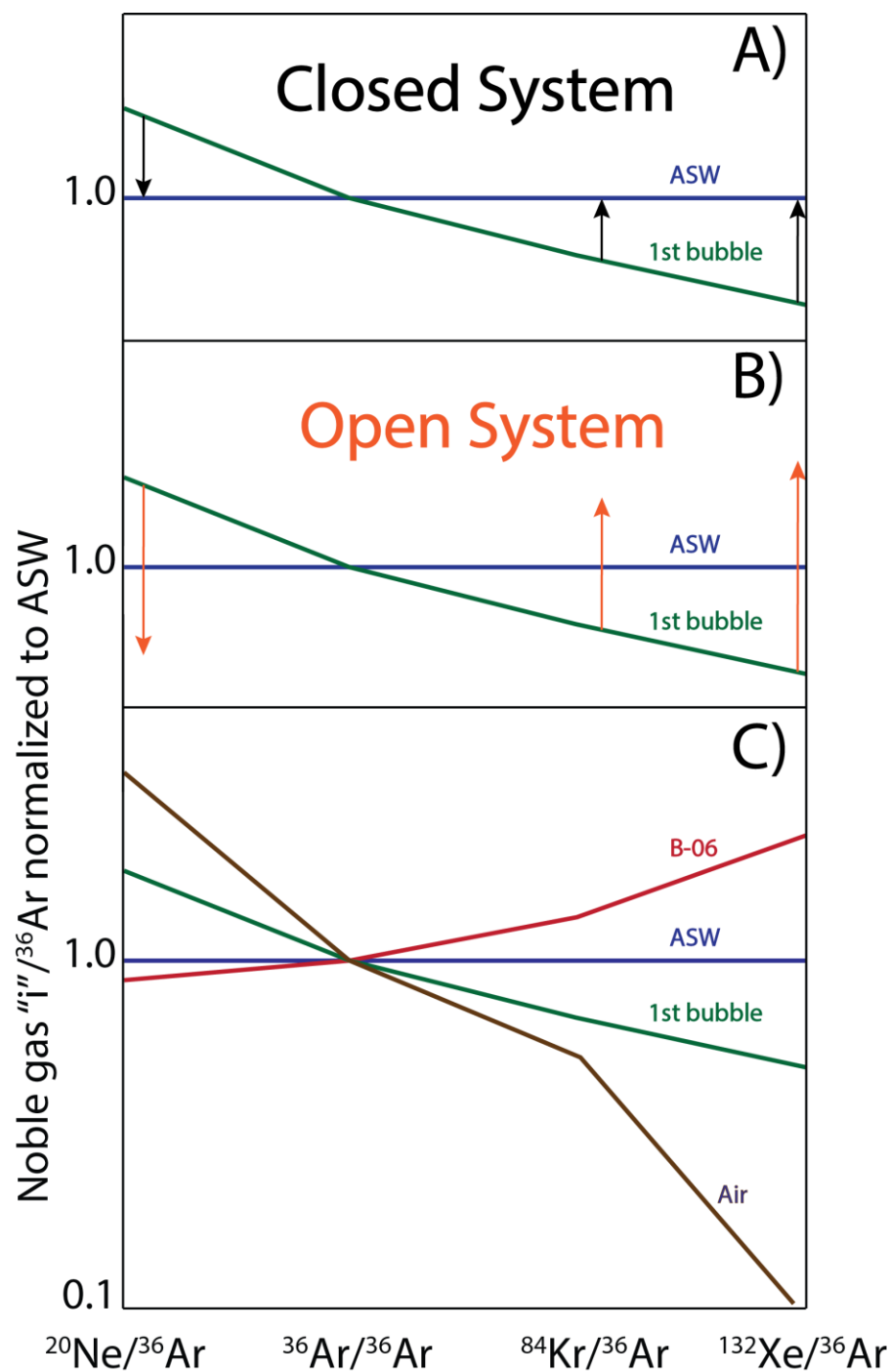


Figure 6 – Spider diagrams: Air-derived noble gas isotope (i.e., ²⁰Ne, ³⁶Ar, ⁸⁴Kr and ¹³²Xe) plotted relative to ³⁶Ar for samples (normalized to ASW); by definition ASW is equal to one. 6a) Hypothetical closed system behavior; 6b) hypothetical open system behavior; 6c) Sleipner results as approximated by sample B-06; notably, ²⁰Ne/³⁶Ar for sample B-06 (considered representative of the system) plots below the ASW line, suggesting open system behavior. In contrast, ⁸⁴Kr/³⁶Ar and ¹³²Xe/³⁶Ar ratios plot well above the ASW line, suggesting that they have been enriched in heavy noble gases (potentially due to interaction with oil and/or sediments). Outlier samples plot very close to air, suggesting significant secondary air contamination (most likely during sampling).

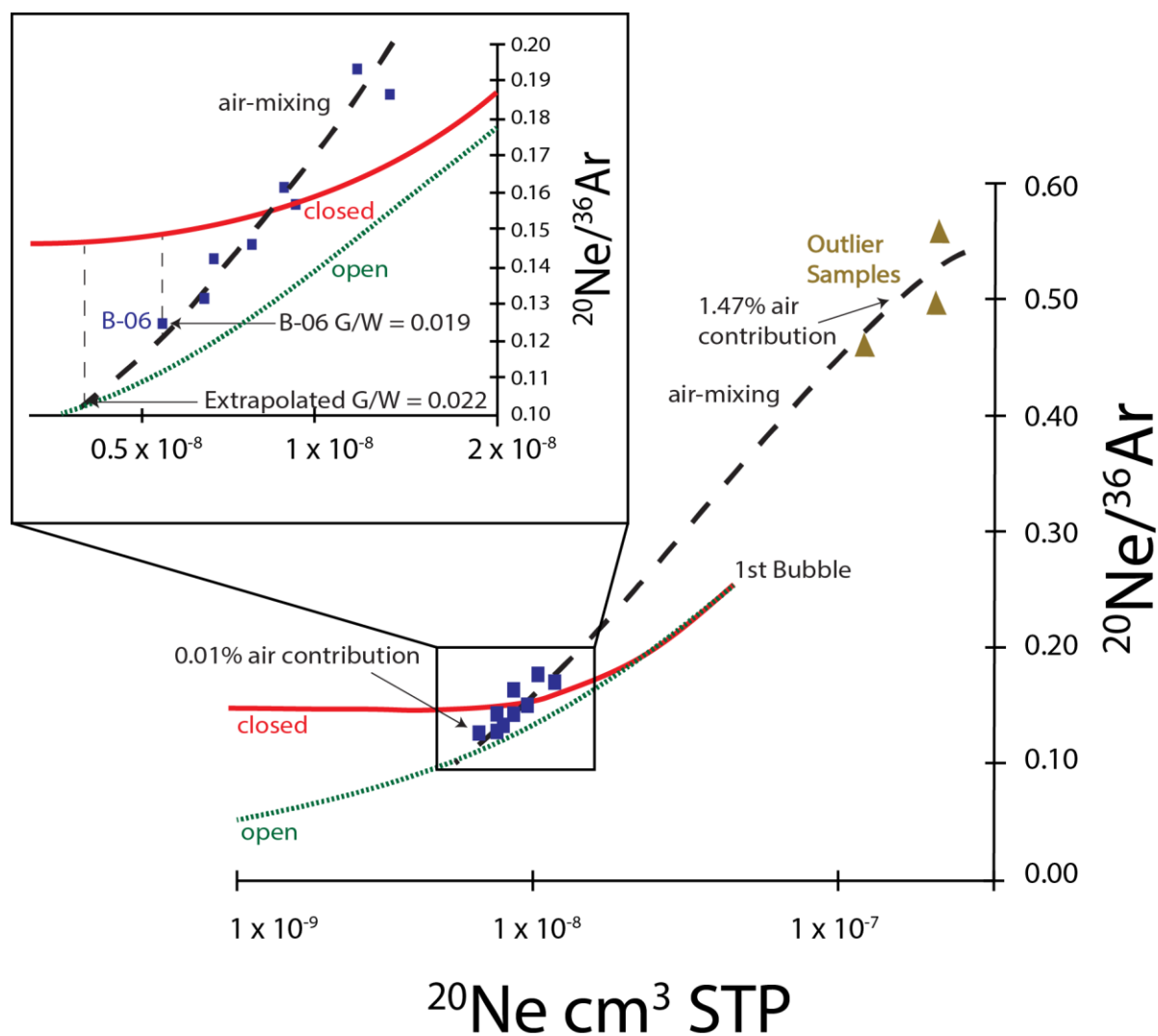
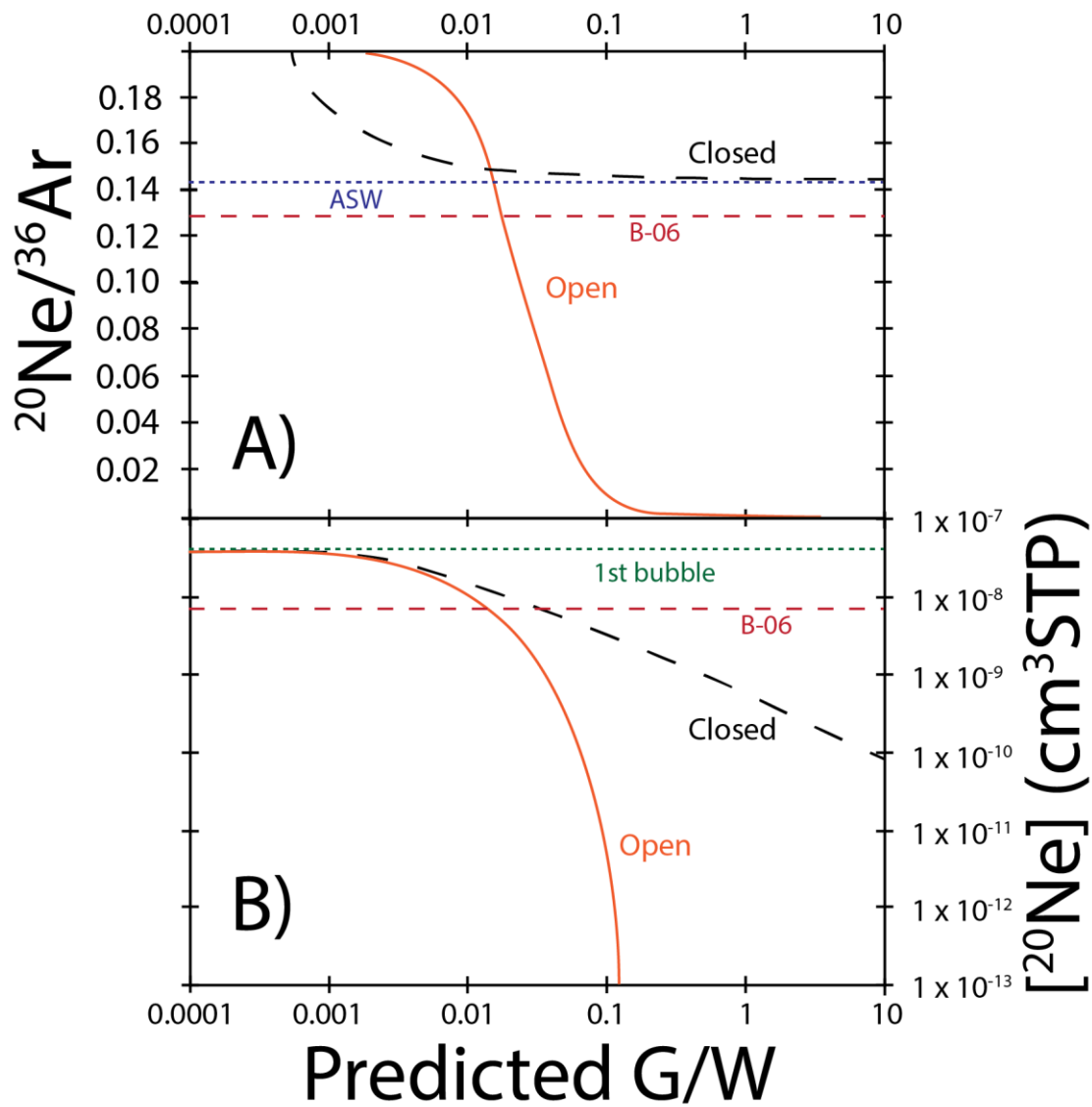


Figure 7 – Ne concentrations vs. $^{20}\text{Ne}/^{36}\text{Ar}$ for Sleipner Vest samples. Normal samples are shown as blue squares, whereas air-contaminated outlier samples are plotted as golden triangles. Closed and open system gas-stripping trajectories are shown as solid red and dashed green lines respectively. Mixing with air is shown as a black dashed line.



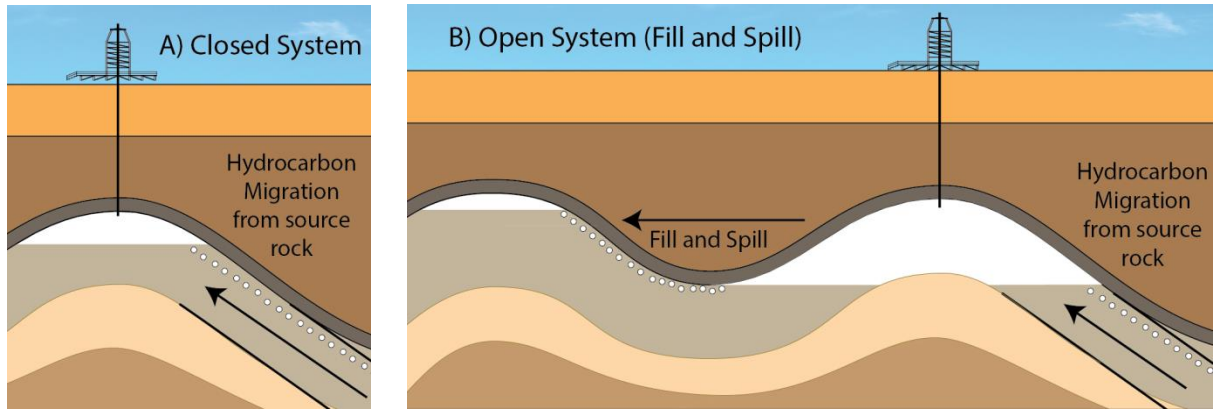


Figure 9a – Diagram showing migration of hydrocarbons (white bubbles) along a fault between two hydrous rock units and filling of a hydrocarbon reservoir (white area). 9b – Diagram showing migration of hydrocarbon bubbles along a fault and filling of a hydrocarbon reservoir and subsequent spilling into an adjacent reservoir.

Table 1. Compositional and stable isotope systematics of Sleipner Vest gases in mole fraction.

Compositions								Stable Isotopes			
Sample	CH ₄ (±2%)	C ₂ H ₆ (±2%)	C ₃ (±2%)	IC ₄ (±2%)	NC ₄ (±2%)	CO ₂ (±2%)	N ₂ (±2%)	δ ¹³ C (CH ₄) (±0.1‰)	δ ¹³ C (C ₂ H ₆) (±0.1‰)	δ ¹³ C (CO ₂) (±0.1‰)	δD (CH ₄) (±1.0‰)
Sleipner Vest											
<i>Outlier Samples</i>											
B02-T1	80.39	7.86	3.65	0.48	0.82	5.35	0.55	-38.0	-28.5	-8.3	-209
B03 T1	70.79	8.37	5.34	1.01	1.98	8.37	0.71	-39.0	-29.2	-7.4	-217
B05 T1	73.67	8.28	4.31	0.58	0.94	10.45	0.79	-39.6	-28.7	-7.4	-221
<i>Normal Samples</i>											
B06 T1	75.93	8.23	4.10	0.53	0.83	8.64	0.75	-39.7	-29.3	-7.5	-218
B11 T1	74.22	8.23	4.21	0.60	0.96	9.23	0.86	-39.8	-28.3	-7.1	-216
B14 T1	74.70	8.24	4.27	0.61	1.01	9.20	0.72	-39.8	-28.7	-7.4	-221
B21-T1	75.14	8.29	4.20	0.55	0.86	9.35	0.74	-39.4	-28.9	-7.5	-215
B07 T1	75.19	8.36	4.26	0.56	0.87	8.93	0.87	-39.6	-28.3	-7.5	-218
B01 T1	69.00	8.28	4.26	0.53	0.82	15.32	0.76	-40.9	-29.1	-7.1	-231
B24-T1	75.93	8.59	4.49	0.60	0.92	7.81	0.84	-40.0	-29.3	-8.0	-217
B13 T1	73.89	8.46	4.57	0.66	1.09	9.42	0.84	-40.0	-28.5	-7.7	-219
B17 T1	73.05	8.48	4.64	0.67	1.07	10.26	0.75	-39.9	-28.0	-6.7	-217
B22 T1	73.76	8.54	4.55	0.62	0.98	9.56	0.83	-40.4	-28.6	-8.0	-220

Table 2. Noble gas (helium, neon, argon, krypton and xenon) isotope systematics of Sleipner Vest gases.

Sample	⁴ He × 10 ⁻⁶ cm ³ STP/cm ³	²⁰ Ne × 10 ⁻⁹ cm ³ STP/cm ³	⁴⁰ Ar × 10 ⁻⁶ cm ³ STP/cm ³	⁸⁴ Kr × 10 ⁻⁹ cm ³ STP/cm ³	¹³² Xe × 10 ⁻¹² cm ³ STP/cm ³	³ He/ ⁴ He (R/R _A)	²⁰ Ne/ ²² Ne	²¹ Ne/ ²² Ne	⁴⁰ Ar/ ³⁶ Ar	⁸⁶ Kr/ ⁸⁴ Kr	¹³² Xe/ ¹³⁰ Xe
Sleipner Vest											
<i>Outlier Samples</i>											
B02-T1	53.7 ± 0.8	239 ± 4	137 ± 2	11.0 ± 0.2	579 ± 9	0.107 ± 0.003	9.74 ± 0.01	0.0289 ± 0.0001	324 ± 2	0.302 ± 0.003	6.58 ± 0.020
B03 T1	57.7 ± 0.9	250 ± 4	161 ± 2	12.6 ± 0.2	710 ± 1	0.110 ± 0.003	9.78 ± 0.01	0.0290 ± 0.0001	315 ± 2	0.306 ± 0.003	6.58 ± 0.020
B05 T1	61.7 ± 0.9	123 ± 2	90.1 ± 1.4	7.61 ± 0.11	526 ± 8	0.112 ± 0.003	9.78 ± 0.01	0.0294 ± 0.0001	338 ± 2	0.307 ± 0.003	6.62 ± 0.020
<i>Normal Samples</i>											
B06 T1	58.4 ± 0.9	7.06 ± 0.11	27.2 ± 0.4	2.94 ± 0.04	338 ± 5	0.107 ± 0.003	9.80 ± 0.01	0.0344 ± 0.0001	488 ± 2	0.307 ± 0.003	6.62 ± 0.017
B11 T1	65.5 ± 1.0	12.6 ± 0.2	30.2 ± 0.5	3.21 ± 0.05	346 ± 5	0.113 ± 0.003	9.82 ± 0.01	0.0326 ± 0.0001	460 ± 2	0.306 ± 0.003	6.58 ± 0.016
B14 T1	63.5 ± 1.0	9.15 ± 0.14	29.0 ± 0.4	3.14 ± 0.05	356 ± 5	0.114 ± 0.003	9.83 ± 0.01	0.0335 ± 0.0001	482 ± 2	0.306 ± 0.003	6.61 ± 0.017
B21-T1	60.4 ± 0.9	8.45 ± 0.13	29.3 ± 0.4	3.71 ± 0.06	376 ± 6	0.102 ± 0.003	9.91 ± 0.01	0.0338 ± 0.0001	487 ± 2	0.306 ± 0.003	6.61 ± 0.017
B07 T1	68.1 ± 1.0	8.54 ± 0.13	28.8 ± 0.4	3.16 ± 0.05	344 ± 5	0.112 ± 0.003	9.70 ± 0.01	0.0335 ± 0.0001	474 ± 2	0.303 ± 0.003	6.60 ± 0.017
B01 T1	53.2 ± 0.8	10.8 ± 0.2	30.9 ± 0.5	3.41 ± 0.05	382 ± 6	0.080 ± 0.002	9.82 ± 0.01	0.0326 ± 0.0001	460 ± 2	0.302 ± 0.003	6.61 ± 0.017
B24-T1	66.4 ± 1.0	14.4 ± 0.2	34.8 ± 0.5	3.72 ± 0.06	410 ± 6	0.104 ± 0.003	9.88 ± 0.01	0.0322 ± 0.0001	451 ± 2	0.302 ± 0.003	6.62 ± 0.017
B13 T1	61.4 ± 0.9	8.43 ± 0.13	30.4 ± 0.5	3.33 ± 0.05	370 ± 6	0.065 ± 0.002	9.79 ± 0.01	0.0341 ± 0.0001	476 ± 2	0.306 ± 0.003	6.61 ± 0.017
B17 T1	66.4 ± 1.0	26.8 ± 0.4	40.7 ± 0.6	4.01 ± 0.06	414 ± 6	0.116 ± 0.003	9.82 ± 0.01	0.0309 ± 0.0001	415 ± 2	0.302 ± 0.003	6.62 ± 0.017
B22 T1	67.2 ± 1.0	10.7 ± 0.2	32.6 ± 0.5	n.d.	403 ± 6	0.112 ± 0.003	9.90 ± 0.01	0.0333 ± 0.0001	470 ± 2	0.302 ± 0.003	6.61 ± 0.017

Table 3. Henry's constants (atm kg/mol) used for gas-water model calculation at various depth, temperature and salinity conditions.

Helium	Neon	Argon	Krypton	Xenon	Depth (m)	Temperature (°C)	Salinity (M NaCl)	Conditions
16.30	13.59	3.77	1.97	1.06	0	10	0.623	Recharge
17.13	17.16	9.42	6.33	4.70	3535	88	1.2	Reservoir
10.45	12.28	7.92	6.35	5.64	5000	180	1.2	Production interval (minimum)
7.00	9.38	5.85	5.37	5.68	6000	250	1.2	Production interval (maximum)

Table 4. Parameters for model calculations

Parameter description	Symbol	Units	Reference
Noble gas species	i, j		
partial pressure of gas	p_i	GPa	
Henry's constant*	K_i^M	Molarity atm kg/mol	
Salinity	S	M NaCl	
Concentration of gas i in the gas phase	$[C_i^g]$	cm ³ STP/cm ³	
Concentration of gas i in ASW	$[C_i^{asw}]$	cm ³ STP/cm ³ H ₂ O	
Total moles of gas i in ASW	$[n_i^{asw}]$		
Degassing steps	d		
Volume of 'gas packet'	G		
Volume of 'water packet'	W		
Air saturated water	ASW		
Discovery reservoir pressure	P_R	Bar	
Discovery reservoir temperature	T_R	Kelvin	
Volumetric gas-water ratio**	$\frac{V_g}{V_w}$		
Density of water	ρ_w		
Lambert transcendental function***	ω		
Subscripts			
initial	0		
At step d	d		
measured	m		

Table 5. Compositional and stable isotope systematics of Sleipner Vest gases.

	G/W (Zero Order)	G/W (First Order)	G/W (Second Order)	G/W (Second Order)
	Complete gas-stripping / Max Value	Equilibrium	OPEN	CLOSED
[²⁰ Ne]	0.071	0.061	0.019	0.071
[³⁶ Ar]	0.062	0.044	0.022	0.059

$[^{84}\text{Kr}]$	0.046	0.019	0.014	0.032
$[^{132}\text{Xe}]$	0.027	-	-	-
$^{20}\text{Ne}/^{36}\text{Ar}$	-	-	0.017	-
$^{84}\text{Kr}/^{36}\text{Ar}$	-	-	0.040	-
$^{132}\text{Xe}/^{36}\text{Ar}$	-	-	0.057	-

Volumetric Gas-Water (G/W) estimates are based on sample B-06, which represents the least air contaminated and thus most representative sample from Sleipner Vest. Dashes are used to denote unrealistic model results (i.e., sample values fall outside of the predicted range). There are no first or second order Xe estimates due to the fact that samples clearly have excess xenon (section 5.4). Recharge conditions: Seawater (0.623M NaCl) at a temperature of 10°C; reservoir conditions: 400 bar; Temperature: 88°C; Salinity: 1.2M (NaCl).